

UNIVERSITÀ DEGLI STUDI DI PADOVA

*Facoltà di Ingegneria*

*Dipartimento di Ingegneria dell'Informazione*

*Corso di Laurea Magistrale in Bioingegneria*

Tesi di Laurea

**ESTABLISHMENT OF THE  
ACTIVE REGION IN SCANNING-MUP SIGNALS**

Laureando: Previato Davide

Relatore: Prof.ssa Sawacha Zimi

Anno Accademico: 2018-2019



# Abstract

Single needle multiscanning EMG is a research technique that provides a new useful way to obtain several motor unit potentials from a single scan. The main issue of this approach is that the solutions are numerous, most of them being invalid solutions presenting only needle cannula pattern or spurious signals linked together.

From the above, the main purpose of this work is to define and test algorithms that are able to estimate the spatial limits of the active region of a motor unit potential and use it to distinguish among valid and invalid solutions. The dataset is provided by single-needle multiscanning-EMG simulations that allow to have a wide variability of records together with the ground truth limits. The proposed algorithms have to achieve two main tasks: discard the invalid signals and set the limits if a valid region of motor unit activity is found.

Three different methods are proposed, described, and evaluated in this work. Results are analyzed for every method and compared between them. Considering only the cases in which a good overlapping with ground truth is available, all of the three algorithms are robust and show an appreciable level of accuracy in their estimation. When comparing them, two of the algorithms show a consistent unbiasedness and a lower error variance than the third one.

## Keywords

EMG, Scanning EMG, Multiscanning-EMG, motor unit, motor unit territory



# Summary

<b>1</b>	<b>Introduction .....</b>	<b>1</b>
1.1	Basics of anatomy and electrophysiology .....	1
1.1.1	Anatomy of the motor unit .....	1
1.1.2	Electrophysiology of the motor unit .....	2
1.2	EMG techniques to investigate MUs .....	3
1.2.1	MUP's extraction from an EMG record. Previous techniques. ....	4
1.2.2	Quantitative-EMG .....	5
<b>2</b>	<b>Scanning EMG .....</b>	<b>7</b>
2.1	Recording setup .....	7
2.1.1	Scanning and Trigger electrodes .....	7
2.1.2	Micro step-motor and scanning corridor definition .....	7
2.1.3	Scanning EMG software .....	8
2.2	Recording procedure .....	8
2.2.1	The procedure .....	8
2.2.2	Interpretation of results .....	9
2.2.3	MU's parameters .....	10
2.3	Signal processing .....	11
2.3.1	Filtering .....	11
2.3.2	MUP activity corridor .....	12
2.3.3	MUP profile .....	12
2.4	Multiscanning EMG .....	13
2.4.1	Classic technique .....	13
2.4.2	Single needle multiscanning EMG .....	14
2.4.3	Multiscanning EMG signals simulation .....	15
<b>3</b>	<b>Automatic detection of MU active region .....</b>	<b>17</b>
3.1	Database pre processing .....	17
3.1.1	Generation of the multiscanning EMG signals .....	17
3.1.2	Linking and ground truth extrapolation .....	17
3.1.3	Quality of solutions. Overlapping description. ....	18
3.2	Active region detection algorithms .....	21
3.2.1	Temporal smoothing approach .....	21
3.2.2	Differential amplitude analysis .....	24
3.2.3	Image segmentation method .....	26

3.3	Auxiliary functions and scripts .....	29
3.3.1	<i>Error finder</i> .....	29
3.3.2	<i>Trace inspectors</i> .....	29
<b>4</b>	<b>Final results and discussion .....</b>	<b>31</b>
4.1	Results of individual methods .....	31
4.1.1	<i>Temporal smoothing approach</i> .....	33
4.1.2	<i>Differential amplitude analysis</i> .....	36
4.1.3	<i>Image segmentation method</i> .....	39
4.1.4	<i>Discussion of results</i> .....	41
4.2	General results .....	44
4.2.1	<i>Initial limit estimation</i> .....	44
4.2.2	<i>Ending limit estimation</i> .....	45
4.2.3	<i>Discussion of results</i> .....	45
<b>5</b>	<b>Conclusions and future trends .....</b>	<b>47</b>
5.1	Conclusions.....	47
5.2	Future trends .....	48
5.2.1	<i>Independent ending limit estimation</i> .....	48
5.2.2	<i>Pattern analysis</i> .....	48
5.2.3	<i>Mask generation</i> .....	49
5.2.4	<i>Real cases analysis</i> .....	49
	Bibliography .....	51

# 1 Introduction

All the signals processed in this work, are related to the functioning of the motor unit during an EMG examination. To analyze this kind of signals it is important to know how they are generated and the way in which they are acquired, distinguishing also normal cases from pathological conditions.

First of all, in this chapter a basic anatomical and physiological structure of the muscle, neuro-muscular junction and motor unit are presented. At last, knowing how EMG signals are generated, the scanning EMG acquisition method is analyzed. This is the basic investigation procedure form which multiscanning EMG was developed in order to simplify the data acquisition. The main advantage of this technique is the possibility to obtain contributions from multiple MUs at the same time using only one needle electrode. Next, the decomposition phases allow to create a wide set of solution.

## 1.1 Basics of anatomy and electrophysiology

### 1.1.1 Anatomy of the motor unit

*Muscles. General features of the skeletal muscle.*

Muscles are complex structures that have contraction capability. They can be divided into three types: *cardiac muscle*, *smooth muscle* and *skeletal muscle*. They can be classified looking at their internal composition or in the way they produce a movement [1].

In the first case, cardiac muscle and skeletal muscle are composed by sarcomeres packed into a regular arrangement that give to them a typical striated appearance. In the second method of classification, cardiac muscles and smooth muscles are grouped as *involuntary muscle*, so they can do automatic contractions. The skeletal muscle, instead, is a *voluntary muscle* type, so it can be activated sending to it a voluntary stimulation via the peripheral nervous system [2].

The skeletal muscle is composed by a large number of substructures. The smallest one, as said before, is the *sarcomere* that consist of filaments of actin and myosin that, by their reciprocal interaction, are responsible of the muscle contraction. The sarcomeres are packaged in a macrostructure called *myofibril*. Connecting myofibrils, a *muscle fiber* is obtained. Also, muscle fibers are organized in larger structures called *fascicles*. All these structures are taken in position by several layers of membranes that can be divided into three groups: *epimysium*, *perimysium* and *endomysium* [2]. Due to their point of anchorage, from a skeletal joint to another via tendons, and their capability of contraction the muscles are responsible of the movements of the body segments.

*Motoneuron and neuro-muscular junction*

The neuro-muscular junction is responsible of the transmission of the electrical stimulus, generated by the brain, in order to command the skeletal muscles movement. It is essentially composed by the

end branches of a *motoneuron*, located in the spinal cord. Every branch reaches approximately the middle of a muscle fiber in a complex of nervous terminal [3]: this zone, where the electrical brain signals are translated into muscular contraction, takes the name of *motor endplate*. A single motoneuron can reach with its branches a large number of muscle fiber so the stimulus due to only one can make simultaneously command all its distal structures connected [2].

### *Motor unit*

The motor unit is the smallest functional unit in the skeletal muscle. It is composed by a motoneuron, comprising its branches and the motor endplates, and finally all the set of muscle fibers connected to it [3].

Looking at the spatial distribution of the fibers along a cross section of the muscle, it is possible to define also the *motor unit territory* as the area in which the motor unit muscle fibers are contained. Along the muscle, the size and the shape of this zone, mainly rounded, is almost preserved. The *motor unit fiber density* can also be calculated giving the number of MU fibers and the area its territory [3].

The motor unit muscle fibers generally run in parallel and are scattered and interdigitated with fibers of other motor units. Although, their spatial distribution inside the territory has become a controversial issue; several tests suggest they are randomly distributed with some degree of clustering [3].

## 1.1.2 Electrophysiology of the motor unit

### *Generation of the muscular activity*

In order to perform a muscular contraction, action potentials are generated by motor neurons located in the spinal cord. The higher the number of motoneurons generating stimulus higher the muscular activity.

Focusing only on a single motor unit it is possible to define all the process involved. First of all, the motoneuron generates the stimulus that propagates through its axon via *cellular depolarization*. The set of discharges takes the name of *motor unit firing pattern* (MUFP) and, in a normal condition, the firing signals are repeated almost periodically in order to generate the complete contraction of the fibers connected. When a MUFP reaches the final branches of the axon is converted, by the neuro muscular junctions in the end plate zones, in acting potentials in the muscle fibers. For every fiber, consequently to a motoneuron discharge, a *single fiber action potential* (SFAP) is generated and propagates in both directions through its. Finally, the *motor unit potential* (MUP) is the resulting signal that takes into account all the SFAPs contributions. By the way, if a MUFP is generated a *MUP train* is obtained and the MU does a continued contraction. It is important, also, to keep in mind that the muscle fibers contraction is always time synchronized with its specific MUFP, related to its specific motoneuron [3].

The complete muscular contraction is, in the end, the result of all the MUs' contractions.



### *MUPs, Behavior and parameters*

MUPs are the most interesting signals in order to know how MUs, so the muscles, are organized. Because a MUP is an electrical signal that propagates through the tissues, it can be detected by an electrode as sum of every SFAP contributions.

The typical SFAP waveform consists in a first low amplitude undershoot under the baseline, a high positive peak and a second low amplitude undershoot. From this curve, several parameters can be detected as the *time duration* of the signal and the *amplitude of the peaks*. Parameters can vary due to fibers' conduction capabilities and geometrical configuration of the electrode-fiber combination; for example, the closer the fibers the higher the amplitudes. In fact, SFAPs generated far from the acquisition zone can be recorded with lower amplitude than the nearest ones. Pathological conditions modify also the MUP behavior [4].

The final MUP signal depends on the shapes of the SFAPs involved but, more importantly, on the exact timing of them. As said before different SFAPs can differ depending on fibers' physical characteristics. The minimal scattering of the endplates generates also potentials a bit further or closer to the electrode position, causing records of signals dispersed on time. Time dispersion is also related to the velocity of conduction on the fibers, higher in the thicker ones [1] [4].

As presented in the last chapter, other parameters can be estimated from the acquired MUP making reference to the *quantitative EMG (Q-EMG)* description [1] [4].

### *Disease conditions*

Myopathic and neurological diseases can reduce the capability of movement in patients with pathologies.

In the case of a *myopathic* disease, muscle fibers are degenerated and their capability of contraction is reduced or completely lost. Inside the MU territory, smaller than the normal, fibers' diameter variability is increased. Only a fraction of the original MU is stimulated by its motoneuron and looking at corresponding MUP, it will be reduced in amplitude and in duration. The complexity of the signal also rises [5].

*Neuropathy* affects the motoneuron-fibers connection. When the axon death occurs the muscle fibers at its end branches are denervated. This condition is, during the time, partially solved by the *reinnervation process*: muscle fibers previously connected with the lost motoneuron are reinnervated by healthy branches next to them, related to other motoneurons. The resulting MUP signal has an increased amplitude, due to the higher fiber clustering, longer duration and higher complexity than normal condition [5].

## **1.2 EMG techniques to investigate MUs**

The acquisition and processing of EMG signals are the two main steps in order to perform feature extraction and classification. The basics of EMG extraction consist on acquisition on a certain

location, where the electrode is positioned, of electrical signals generated by MUs. The next generation methods, as scanning EMG, are able to perform acquisition in multiple locations, giving also information about the spatial position of the signals being generated. These kind of approaches are very useful in order to have a more complete information of the muscle under investigation.

### 1.2.1 MUP's extraction from an EMG record. Previous techniques.

#### *Electrodes*

As every biomedical signal, EMG needs to be acquired by electrodes. In the EMG field it is possible to distinguish mainly between *superficial electrodes* and *needle (or intramuscular) electrodes*.

The formers are used in several application, as sport medicine, because are not invasive, their main advantage. In the other hand, due to the tissue dispersion and a low spatial selectivity, they cannot provide a fine estimation of the MUs involved in a muscular contraction [4].

Needle electrodes are commonly used in clinical EMG exams due to their capability to acquire signals directly in the site of the MU to be investigated, reducing also the noise and the tissue dispersion. They are, in opposition to the superficial ones, invasive. The type of needle electrode most used commonly in clinical EMG examination is the *concentric* one. It is composed essentially by three parts: the external cannula, an insulating layer and an inner metal core. Typical materials and size parameters of this kind of electrode, used also in scanning EMG, are reported in the next chapter [1] [4].

#### *EMG's study protocol with needle electrode*

In order to record the EMG signal, an acquisition protocol must be followed. It consists of four phases: first of all, in *the insertion activity* the needle electrode is inserted into the relaxed muscle. During this phase a small discharge of potential is generated, although it has a low diagnostic value.

Then, the muscle is studied during its *activity at rest* moving also the electrode in order to search muscular activity. In this situation, normally, a muscle is electrically inactive. There are only two activities than can appear: the *endplates noise* and the *endplates potential*. In a pathological case can also be recorded *fibrillation potentials*, *positive waves*, *fasciculation* and other spontaneous activity.

In the third phase the muscle is studied under a *slight voluntary contraction* where only few MUs are recruited. The signal recorded shows MUPs scattered in time and as the force increases the number of MUs recruited increases making the analysis of the individual MUP signals more difficult. At this level, the MUP signals can be extracted, processed and classified looking at features as amplitude, duration and number of phases. The skeletal muscle differs in its inner structure so, in this kind of protocol, the needle electrode needs to be moved and reinserted in other positions in order to have a more detailed characterization of the activity of different MUs.

At last, a recording during a *maximum voluntary contraction* is performed. The main goal in this phase is to identify the *interference pattern (IP)*: when the muscle activity increases up to the maximum the number of MUs being activated is very high and it is impossible, in normal conditions,

to distinguish between different MUPs. In this case, the analysis relies on techniques as the turns/amplitude analysis, focusing on characterizing the complexity of the signal.

### *MUP's extraction*

Since MUs are spatially superposed in the muscle, their MUPs will also be superposed, in an EMG recording. In particular, MUPs are repeated in time due to the synchronization with their respective MUPP. Hence, MUPs from different MUs can interfere in time whenever two or more MUs are firing close in time. This behavior makes the MUP's identification process not easy to perform.

Trying to extract MUPs generated by the same MU, temporal windowing and aligning method were used in the past without useful results. In particular, the needle electrode had to be placed in 4 or 5 different locations and for everyone of it an acquisition up to 10 MUP signals [1].

More recently several methods were used to resolve this classification issue and can be grouped into *manual methods* and *automatic methods*. Manual methods are less used because their incapability to adapt to changes in MUPs behaviors. They are also time consuming and need to be used by expert and well-formed personal. Automatic methods are, instead, commonly used for the decomposition problem. In particular, *multi-MUP methods* seem to provide good results in this field and their main advantage consists on a system that can identify all the MUs' firing potentials: starting from the EMG signal, MUP waveforms are identified and analyzed ensuring the discharge isolation of every activated MU. This automatic ability to discriminate between superimposed MUPs allows the user to calculate easily the signals parameters reducing also the time spent. Also in this case, the technique needs the reinsertion of the needle electrode in different locations of the muscle in order to produce a better estimation of MUs activity [1].

### *Multipoint EMG techniques*

*Multipoint techniques* were developed in order to record MUPs information simultaneously in different spatial locations, avoiding the needle electrode reinsertion. In these cases the electrode configuration changes: along its cannula a set of electrodes is positioned generating a recording corridor. During an EMG investigation the needle is inserted perpendicular to the muscle fibers. When the acquisition is performed, it is possible to record information along the cross-section of the MU territory being studied, in multiple location at the same time [2].

### 1.2.2 Quantitative-EMG

*Quantitative-EMG (Q-EMG)* is a valid method of classification of the features of an EMG signal. Its main objectives are to assist the diagnosis relying on accuracy and transparency factors. The first of the two has the purpose to characterize the status of the muscle under examination, in correlation with the overall clinic patient history. The transparency is also fundamental because allows the operator to have an understandable and standardized method that describe a particular muscle condition.

Q-EMG can be performed following different methods, grouped mostly in the two categories of time and frequency domain analysis. The one presented hereafter it is based on the extrapolation of characteristic MUP parameters and find direct implication on this Thesis.

So, relevant Q-EMG parameters on the time domain are defined once the MU territory is isolated, and they are:

- *Baseline*: constant signal representing the electrical zero or the mean value of the signal recorded in a temporal window. Once estimated it is subtracted to the MUP in order to calculate the other parameters.
- *Duration*: time interval between the start of the first depolarization and the end of the last repolarization. It includes the main spike and usually it is also taken in the extremes points in which the potential cross the baseline, through this is not always a valid method.
- *Amplitude*: peak to peak voltage within duration. It provides information about the diameter of muscle fibers, their distance from the scanning needle and of the time scattering of fire potentials. It depends on filtering methods applied.
- *Area*: integral of the rectified MUP signal over its duration. It allows to estimate better the muscle activity than the amplitude.
- *Spike duration*: time interval between the first and the last positive MUP's peak.
- *Spike area*: integral of the rectified MUP signal over its spike duration.
- *Number of phases*: number of baseline crossings plus on the duration. Healthy subjects have usually no more than three phases. An increment of this number can be related at the SFAPs temporal dispersion. It is called *polyphasic potential* a MUP that have more than four phases.
- *Number of turns*: number of positive and negative peaks separated by a fixed amplitude threshold. It is called *complex or serrated potential* a MUP that have more than five turns.
- *Satellites*: small potentials, related to single fibers time-locked to the main contributions, appearing out of the duration interval.
- *Thickness*: ratio between area and amplitude. It is more sensitive than duration to discriminate between normal and myopathic conditions and also less sensitives to the electrode position.
- *Size index*: calculated as two times the logarithm of the amplitude and summed to the thickness. It is an optimal combination of MUP parameters and remains stable when shifts of the electrode occur.
- *Electromyographic jiggle*: describe the variabilities introduced to the MUP if the SFAPs are scattered in time. This parameter increases in presence of neuropathies.

## 2 Scanning EMG

The main issue in a standard EMG study is the difficulty to have a look at the spatial characterization of the muscle. The needle also has to be moved in different positions and it can be painful for the patient. Scanning EMG, taking also the advantages proposed by multipoint techniques, try to solve these points giving a new way to represent the activity into the muscle. Briefly, in this method the recording electrode is inserted in position and acquisitions are taken step by step pulling out the needle. In order to distinguish between signals produced by different MUs, also a trigger electrode is used. Finally, a signals post processing is needed.

### 2.1 Recording setup

#### 2.1.1 Scanning and Trigger electrodes

As described in the chapter 1.2.1, needle electrodes are the most widely used electrodes in order to record EMG. They can be inserted next to the source of interest avoiding interferences and signals dispersion on tissues.

In a scanning EMG record two needle electrodes are used. The one that makes possible the acquisition of the MUPs signals is called *scanning electrode* [3]. It has a concentric configuration: an inner metal core (platinum or stainless steel, diameter: 0.10-0.15mm), an insulating layer and, outside, a metal cannula (stainless steel, diameter: 0.5mm). The distal edge of the electrode is angled, thus the surface acquisition area is elliptical (angle of cut: 15°, caption area: 0.07mm<sup>2</sup>). The core and the cannula are then connected to a differential amplifier to perform the EMG records [1].

The second needle electrode used is the *trigger electrode* and it allows to acquire the MUFPs, generated by motoneurons, at the endplates level. It consists on a metal cannula and a metal core, separated by an insulating material, exposed only in a small rounded recording area on the side (diameter: 25µm, position: 7.5mm from the tip of the cannula). This high sensibility to single fiber is useful in order to know when the MU under study is activated, making possible the EMG decomposition [4].

#### 2.1.2 Micro step-motor and scanning corridor definition

After the scanning needle, and also the trigger one, insertion and since it has a single recording site, it needs to be pulled off from the muscle in a specific way. To do this a micromotor is used: at every control signal it extracts the electrode by a predefined distance (50µm). So, the resulting scanning corridor is defined as the set of spatial positions in which a record is done [3].

### 2.1.3 Scanning EMG software

Analog signals acquired are amplified, digitalized and sent to a computer in which a specific scanning EMG software is installed. Its most important task is to define a threshold for the trigger electrode's signals. When the EMG signal exceeds the threshold imposed, the software has to start its routine. First, it records the EMG, through the scanning electrode, in a predefined temporal window. Then, in

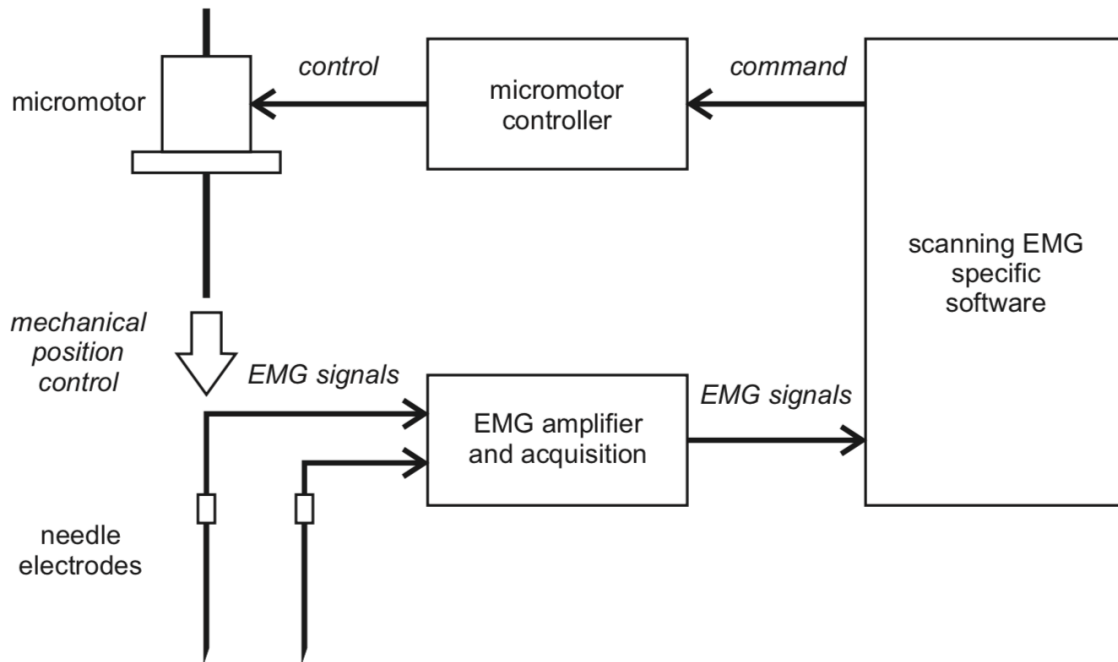


Fig. 1. Scanning EMG system (extracted from [3]).

order to move the needle a control command is sent to the micromotor. At last, the software waits for another trigger event and repeats the previous phases [3].

## 2.2 Recording procedure

### 2.2.1 The procedure

The first step of the investigation process is the insertion of the trigger electrode. It has to be positioned in a location in which a stable waveform is recorded during a slight voluntary contraction. Once the signal recorded has a good amplitude and it is not affected by other MUs contributions, the needle electrode has to be maintained in position preventing further modifications in the recording. Also, the voltage threshold must be adjusted to a level that ensures a single trigger event whenever the MU under study is stimulated.

The second phase consists of the insertion of the scanning electrode. It is, first of all, positioned beside the trigger one (recommended 20mm) along fibers direction and next inserted as perpendicularly as possible into the muscle. The needle is then pushed inside, looking for time-locked signals with the trigger pattern with high amplitude and slow rise time too; if these conditions occur the MU territory

is reached. Needle electrode finally has to be pushed till reaching a zone in which no more spike signals are detected.

At this point, with the trigger electrode fixed, the connection between scanning electrode and step-motor is done. So, the recording procedure can be started: at every control signal the step-motor pull out the needle and the acquisitions are performed in every position of the scanning corridor. The complete procedure takes at least five minutes [3].

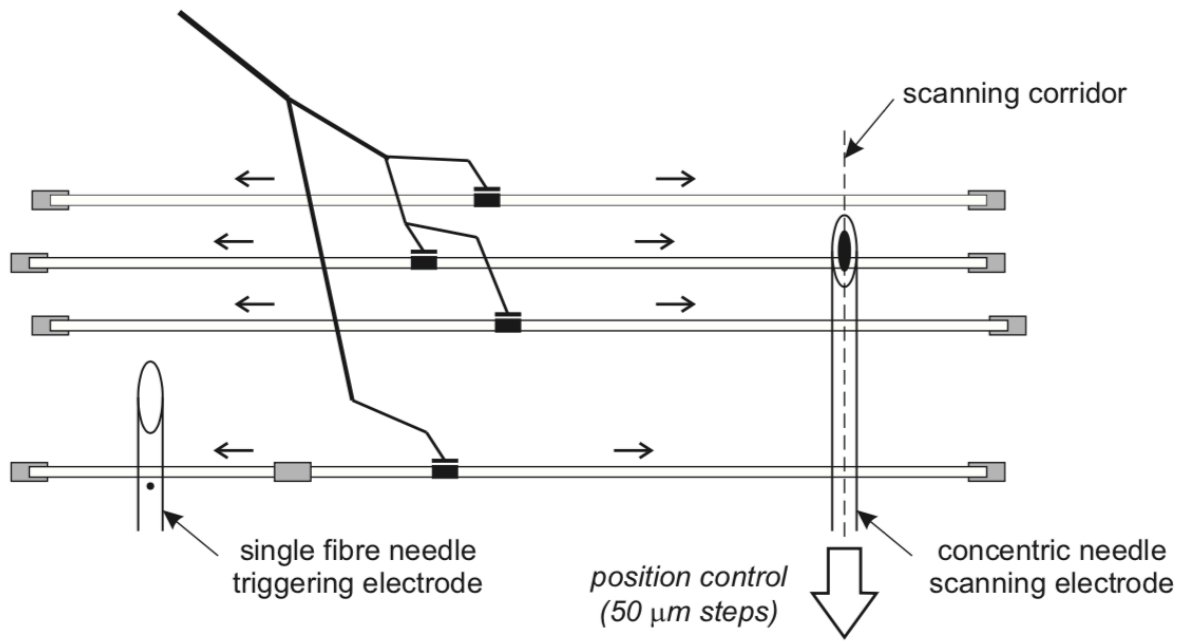


Fig. 2. Schematic representation of a scanning EMG procedure (extracted from [3]).

## 2.2.2 Interpretation of results

The results of a scanning EMG examination are recorded finally in a 2-dimensional structure of data. One of the two represents the temporal domain discretized in time, the other represents the spatial position, as an increment index, in which every acquisition was done. So, every cell contains the MUP's amplitude at the  $i$ -th time instant and  $j$ -th space position. This matrix can be seen also as a level map: hills, valleys and a color scale allow to have a complete characterization of the whole signals under study. In particular, regions in which MU's activity is high are called *motor unit fractions* and are, in general, separated by *silent areas* at low activity [3].

Analyzing a standard spatiotemporal distribution, it is possible to identify three main zones: *cannula zone*, *MUP zone* and *superficial zone*. In the first part of the acquisition the scanning electrode, at maximum depth, is too far from the MU territory so SFAPs are not recorded, although, a negative low amplitude and almost constant pattern is acquired. This fact is due to the cannula's negative polarity given by the connection with the instrumental amplifier. During the pulling of the scanning electrode its active area approaches to the MU territory and an inversion of the signals can be seen. The MUPs zone is characterized by one, or more, positive hills and singles MUPs at different depth have their typical shapes, with a different gain in amplitude. In this case cannula's contribution is avoided. When the electrode's tip goes outside the MU territory the electrode continues to catch the last MUP due to its angled shape. The third zone, nearest the surface, corresponds to the positions

in which the needle is completely outside of the territory. Also, cannula cannot produce its typical pattern because it is outside of the skin [3].

From this knowledge on the data structure, several parameters can be estimate on single MUPs or on the whole MU recorded. In order to extract MU territory, discarding interference contributions as the cannula one, automatic evaluation methods can be used, main objective of this Thesis.

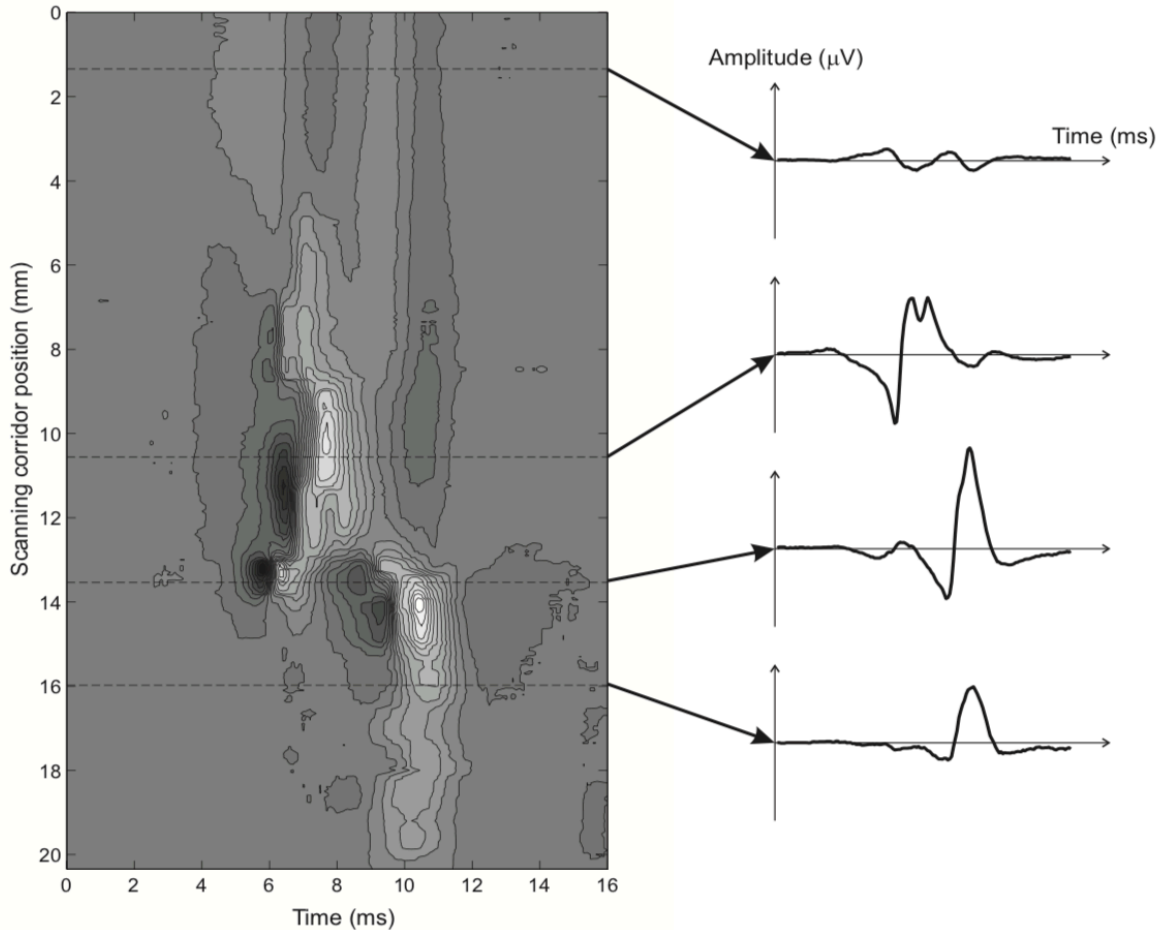


Fig. 3. MUP as level map. On the right the representation of the signals in characteristic locations (extracted from [3]).

### 2.2.3 MU's parameters

Once the MU's territory is defined, it is possible to have a better look at the possible internal configuration of it. As said previously, single MUPs can be extracted from the spatiotemporal matrix, focusing on a single spatial location. This approach is referred as Q-EMG.

MU can be described with global parameters [3] [6], well represented in the data matrix map. They are:

- *Length of the MU cross-section*: defined as the maximal distance between traces with amplitudes at least  $50\mu\text{V}$  or alternatively as the length between the two most distant traces with amplitudes above 15% of the maximum positive amplitude of the scan.
- *Number and length of silent areas*: defined as the number of areas within the length of a motor unit cross-section with amplitudes below  $50\mu\text{V}$ . Their length is measured over the cross-section of their region.



- *Number and length of fractions*: defined as the number of areas within the length of a motor unit cross-section with amplitudes above  $50\mu\text{V}$ . Their length is measured over the cross-section of their region.
- *Number and length of polyphasic fractions*: if more than 4 phases or more than 5 turns are found in a MUP it is defined as polyphasic. So, fractions containing this MUPs behaviors can be counted and measured in length.
- *Temporal dispersion of motor unit fractions*: defined as the latency difference between the earliest and the latest MUP traces recorded within a motor unit cross-section.
- *Depth of the motor unit territory*: from scanning EMG's records also this parameter, not appreciable in normal EMG investigations, can be calculated. Methods that use stereotactic reconstruction or take information from the contribution of the signals, within the length of the cross-section, provided an estimation of the spatial position of the MU. Automatic algorithms that try to resolve this issue are presented in next chapter.

## 2.3 Signal processing

### 2.3.1 Filtering

Every signal is affected by noise when recorded. Filtering is the first process that is commonly performed and there are different methods to be applied. In the case of scanning EMG two different filters are used: *band pass filter in the time domain* and *median filter in the spatial domain* [6].

The first one is applied just after recording in a specified spatial position ensuring the removal of the baseline effect at low frequencies and the interference components at high frequencies. After, the temporal summation of several raw MUPs, recorded for every MUFP generated, can be done to obtain a stable and clear waveform [6].

When the scanning procedure is ended and the data matrix is completed, a median filter is applied on the spatial dimension, so along the scanning corridor. This procedure allows to reduce the effects of others superimposed MUs potentials, but not synchronized in time, with the ones want to be recorded. The number of points filtered at the same time by the median filter are up to 7 and a reduction of the peaks can be also obtained up to 30%. Taking into account this drawback, this second approach can clean the Scanning EMG record in an appreciable manner, neglecting all the artifacts [3].

Median filtering in spatial domain is simple to implement, although the output amplitudes may present a stepped behavior. A more complex procedure can be used based on a least-square smoothing to solve this issue (Fig. 4). In essence, the reconstruction in every spatial position is done on the knowledge of the residual obtained from the construction of a stable MUP, by summing several MU's discharges. A weighting matrix can be calculated and applied to the raw signal in order to smooth it. The results of this method are more similar to the noise-free version of the scanning EMG, maintaining the shapes of the positive and negative surfaces [6].

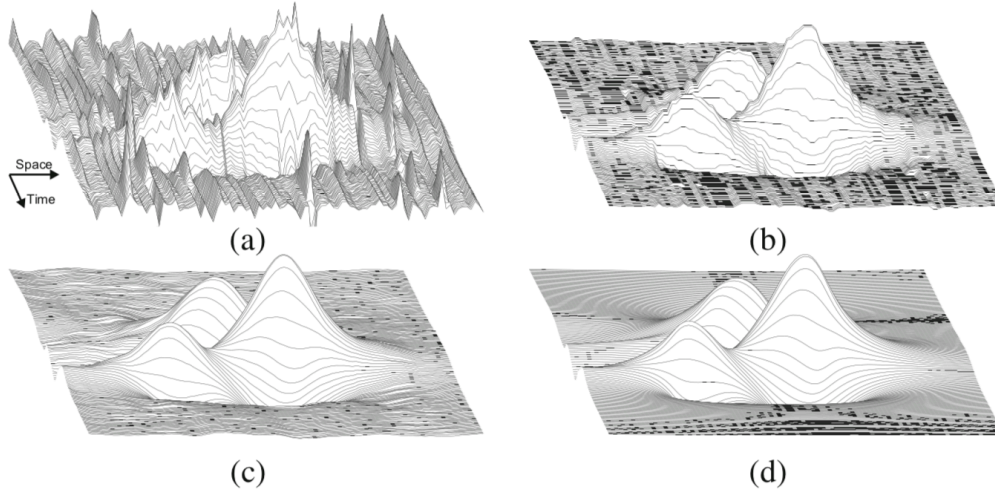


Fig. 4. Effect of spatial filtering. (a) Raw signal. (b) Application of a 7-points median filter. (c) Application of the least-square based filter. (d) Ideal noise free MUP (extracted from [6]).

### 2.3.2 MUP activity corridor

When a MUP is detected from the trigger electrode, some acquisition systems can perform a record taking into account a time interval larger than the one in which a MUP is contained. So, in these cases the detection of the *activity corridor* is important to have a look at the correct temporal window of the signal avoiding also the possibility to record others MUs' interferences.

One of the algorithms that can be implemented starts with a noise reduction, performed also with a *wavelet transform*. After, it calculates the cutting location of the corridor using an innovative way: MUPs are summed in spatial dimension and the autocorrelation function, of this output signal, is calculated. Then, considering a thresholding, peaks and minimum are detected and they give information about the width of the corridor [5] [7].

Nevertheless, this technique is not implemented in this Thesis due to the data generation presented in chapter 2.4 and 3, that already describes the MUP signals included in a fixed temporal window.

### 2.3.3 MUP profile

The map obtained by the previous phases can be processed providing a different characterization of the scanning EMG signal. From the smoothed map new parameters referred to amplitude can be calculated based on a point tracking algorithm.

The algorithm is mainly composed by two steps. The first phase consists on extracting the information about the *turns* of every MUPs that composes the whole record. A turn is essentially a change in the waveform's slope from negative to positive or vice versa. Only the changes that over a certain threshold fixed are considered as turns, in this case [7].

After that, a point tracking algorithm is used to join in the spatial dimension turns of the same sign and close enough in time. During its running, another threshold and a greedy exchange algorithm are used to discard the possibility to join points that are crossing a turns line of the opposite sign. Finally, an additional step can remove traces with length less than a certain value [7].

The results obtained give information about two new projection of the scanning EMG record. On the space-time plane it is possible to observe the traces estimated and their relative temporal delay (Fig. 5a). Every positive trace is followed, or preceded, by a negative one: from this prospective it is possible to make a raw visive estimation, for example, of the cannula-MU transition looking at the inversion of the positive-negative pattern, as said. On the space-amplitude plane, instead, the changes in amplitude of the projected hills and valleys of the map (Fig. 5b). Also in this case, with a simple visive estimation, it is possible to detect in a raw manner the MU territory looking at the very large increment in amplitude of the curves [7].

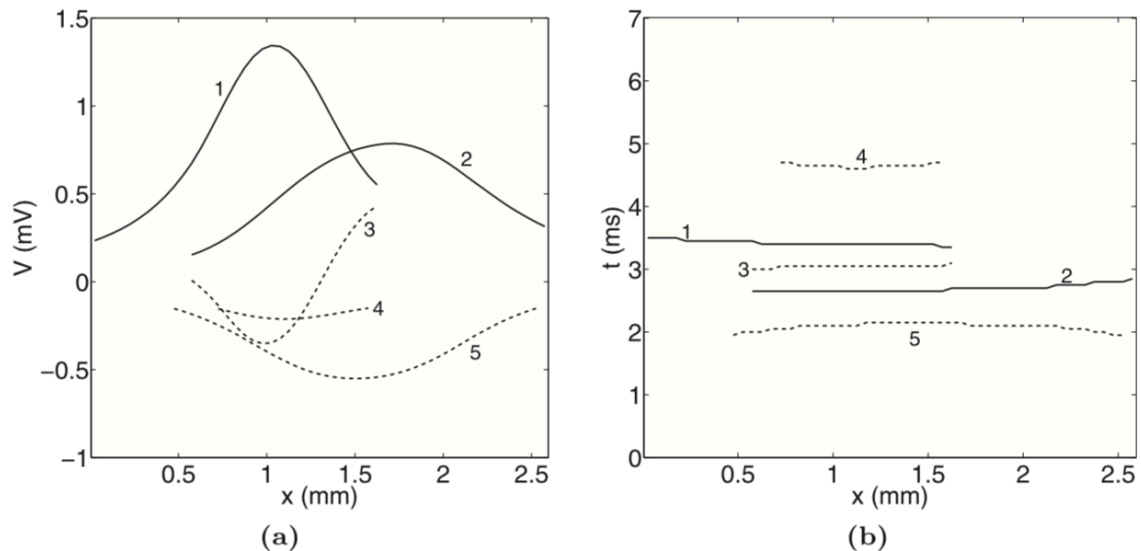


Fig. 5. Representation of MUP projections. The solid lines correspond to positive linked turns, the dotted ones to the negatives. The correspondence between lines is given by the numbers. (a) Space-amplitude projection. (b) Space-time projection (extracted from [7]).

## 2.4 Multiscanning EMG

Scanning EMG technique allows to get information about a single MU. This is possible due to the high selectivity of the single fiber trigger electrode. In order to analyze contributions from other MUs, this electrode needs to be repositioned in the vicinity of another MU territory to record its firing pattern and timing the acquisition system. This limitation is solved by *multiscanning EMG* [8].

### 2.4.1 Classic technique

The main change from the previous scanning method is to use a different trigger methodology, e.g. using a set of fine-wire ones [9], with the purpose of detecting multiple firing potentials belonging to multiple MUs. In order to distinguish between different MUFPs, the signals detected are decomposed, using a waveform classification method.

Consequentially, the acquisition electrode is not pulled out depending on the command generated by the trigger one: for every spatial position, an acquisition is performed in a predefined fixed time

interval (variable from 300ms to 1s). At the end of this process, not MUPs but EMG signals are recorded by the scanning electrode.

Finally, the trigger decomposition ensures to detect MUPs of each different MU and separates solutions in multiple records. The extraction of these signals is achieved by windowing the EMGs records in each spatial position, depending on a specified MU fire pattern. Once obtained multiple raw MUPs the temporal mean of them is taken as resulting signal, improving its representation. In essence, this is a spike-trigger averaging method.

The matrices of data obtained have the same characteristics of the scanning EMG ones, with the advantage that multiple MU contributions are identified during a single insertion of the electrodes.

### 2.4.2 Single needle multiscanning EMG

The information about MU activity can be redundant using both trigger and scanning electrodes. Single needle technique wants to solve this problem placing in only one electrode the responsibility to identify MUFPs and to acquire EMG signals at different depths. The electrode used is the concentric one due its characteristic to record potentials from a wider area.

For each spatial location, the EMG signal is acquired and decomposed (Fig. 6a-6b). The extraction of the MUFP allows, as in the classic method, to superimpose time windows on the recorded signal. For each discharge pattern, the temporal mean of the MUPs detected is calculated in order to obtain well-defined waveforms.

Final scanning results for different MUs are obtained matching the same firing event-related potentials along the spatial position. A greedy-exchange based algorithm is implemented to reach this objective (Fig. 6c). At the end, the obtained signals represent MU contributions at different depth with a variable number of traces. Hence, unlike the scanning EMG technique, the solutions could not cover the whole spatial dimension of the scanning corridor. It can also be possible that a single MU or its fractions are being represented on multiple solutions or that solution presents a negligible zone, such as the cannula one.

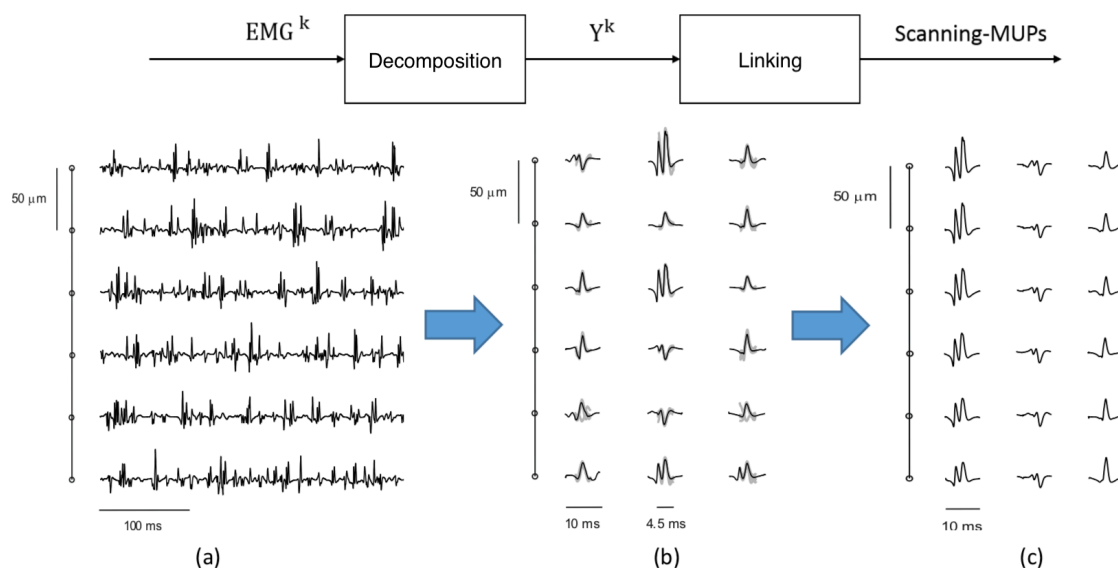


Fig. 6. Scheme of multiscanning-MUP recording. (a) EEG recorded for each position by the needle electrode. (b) MUP decomposition for each position depending on different MUs. (c) MUP generation by linking procedure (extracted from [8]).

### 2.4.3 Multiscanning EMG signals simulation

Simulation is the way in which estimation results can be compared with ground truth. This phase, in particular for this thesis, is fundamental in order to work on a wide dataset, verify the validity of the algorithms implemented and extract errors. Multiscanning EMG data are generated taking into account three main models: *muscle model*, *recruitment and firing model* and *EMG model*.

#### *Muscle model*

Muscles are modelled with a circular cross-section with a radius of 7mm and each one contains in total 120 MU. The whole muscle cross section area is initially superimposed by a grid of points, taken as possible centers of the territories. MUs are distributed in the muscle depending also on their degree of overlapping, expecting it to be as constant as possible in different locations of the muscle. The area of the territories is modeled as an exponential function, obtaining values between 1.96mm<sup>2</sup> to 22.48mm<sup>2</sup>. Density of fibers is constants for all MUs, so their number in each territory only depends on its area, following an exponential behavior. Hence, the number of fibers can vary from 50 to 200 for smaller and bigger MUs respectively. Fibers length is set to 140mm.

The conduction velocity can vary between fibers, depending on their diameter and physical properties. This factor is described as a gaussian distribution, for every MU, with a standard deviation of 0.1m/s and a mean variable depending on the territory size. So, conduction velocity can vary from 3.25m/s to 6.25m/s.

Usually, a MU is divided in fractions. This characteristic is simulated overlapping a hexagonal cells grid on the whole muscle cross section. Each cell represents a fraction and their number, depending on the area and location of the territories, can vary for different MUs. Next, fibers are divided in their corresponding fractions according to their proximity to the centers of the cells.

Once defined this subdivision, the innervation zone for each MU is described. Its center corresponds to the mean point of the fibers set length and from this, centers of innervation of the fractions are deployed in a 10mm wide zone. Consequentially, endplate zones are spatially scattered by 1mm from the center of each fraction.

#### *Recruitment and firing model*

MUs are recruited depending on the percent of the *maximum voluntary contraction (MVC)* imposed. Recruitment is also defined with an exponential curve, *recruitment threshold excitation (RTE)*, that correlates it with the number of MU in the muscle. Results of this model show that smaller MUs are the firstly recruited and their number increases exponentially depending on the MVC. In particular, the percentage of MUs recruited is higher at low levels of MVC.

Firing rate of every MU depends on the type of muscle considered. Modeling it with an appropriate function, taking into account also the MVC contribution, it is possible to notice that the firing rate is higher in the MUs recruited in the first phases of contraction.

From this knowledge, the MVC is taken in the range from 2% to 4% hence, the maximum number of MU recruited is 19 and 39 respectively. Consequentially, the firing rate ranges from 9 discharges/s to 11 discharges/s.

### *EMG model*

The EMG signal recorded is finally simulated by the summation of every SFAPs generated in proximity of the electrode' detection area. Moreover, the cannula contribution is subtracted: this is modelled as a mean of the potentials recorded in multiple points along the electrode case.

A simulated procedure consists in the insertion of the scanning needle through all the cross section of the muscle, in a central position. The scanning corridor is determined pulling out the electrode by 50 $\mu$ m after every record. Depending of the muscle diameter the spatial dimension of the data matrix is composed by 280 lines. The duration of every record can vary from 500ms to 1000ms with a sampling frequency of 20kHz.

<i>Model</i>	<i>Model parameters</i>	<i>Parameters value</i>
<i>Muscle model</i>	Cross section radius	7mm
	Number of MUs	120
	Territory area of MU	[1.96, 22.48]mm <sup>2</sup>
	Number of fibers/MU	[50, 200]
	Fibers length	140mm
	Fibers conduction velocity	[3.25, 6.25]m/s
	Muscle innervation zone wideness	10mm
	Fractions innervation zone wideness	1mm
	Fat layer thickness	2mm
	Skin layer thickness	1mm
<i>Recruitment and firing model</i>	MVC	[2, 4]%
	Number of MUs recruited	[19, 39]
	Firing frequency	[9, 11]fires/s
<i>EMG model</i>	Spatial recording samples	50 $\mu$ m
	Temporal duration of record	500ms – 750ms – 1s
	Sampling frequency	20kHz

Tab. 1. Models parameters and values [8].

## 3 Automatic detection of MU active region

Scanning EMG provides a wide set of data useful for the further analysis on parameter estimation. It is possible, as said, to get information about individual MUPs, extracted from the rows of the record matrix, or on the whole MU, taking into account also the spatial information through columns. [8]

With this powerful technique it is possible to process in different manners all the signals of interest and setting up automatic methods to estimate the spatial location, so the territory, of the active MUs into the muscle. After that, the generated MUPs can be studied using the Q-EMG techniques.

### 3.1 Database pre processing

#### 3.1.1 Generation of the multiscanning EMG signals

The algorithms presented in the next sections need to be evaluated in different scenarios, ensuring the possibility to cover almost all the variabilities recorded in real conditions. In order to do that, multiscanning EMG signals are simulated and stored in MatLab files thus, a bench of data with the desired grade of diversity between MUPs was created.

The database contains two types of files. The simulation ones contain the ground truth MUPs accompanied with the set of MUs parameters used for their generation, as described in 2.4.

The multiscanning EMG solutions are stored in files related to the previous ones according with the number of trials and the MVCs. The number of signals stored in these files are higher in number than the simulation ones. In fact, not always a solution can represent a well overlapped MU's territory due to the generation of the data.

All these files have been provided as starting point for this thesis work.

#### 3.1.2 Linking and ground truth extrapolation

Into the multiscanning EMG files, there are also variables that allows to link the records to their ground truth. However, the number of MUPs successfully matched can be lower than the entire number of solutions. In fact, if a signal has a low number of traces, has small amplitudes or it is very noisy (condition that can occurs when the MVC grows up), the linking algorithm cannot find a match with the corresponding MU contribution, so ground truth is not available. Consequently, the number of MUs evaluated can be lower than the expected.

When a scanning-MUP is matched with its reference, MU territory limits can be extracted following two methods:

- *Fibers contribution*: it takes into account the electrical influence region of the fibers located inside the physical limits of the MU territory. If the scanning corridor crosses this region, or it is very close to it, the resulting ground truth depends on the higher and the lower spatial

samples in which the fibers maximal zone of conduction starts and ends. This is the approach that describes in the better way the real acquisition conditions (Fig. 7a).

- *No fibers contribution*: the physical MU limits are considered as ground truth. This method wants to imitate the possibility that the acquisition zone is far from the MU territory. In this case, the signals recorded are too low to be considered as representative for further analysis (Fig. 7b).

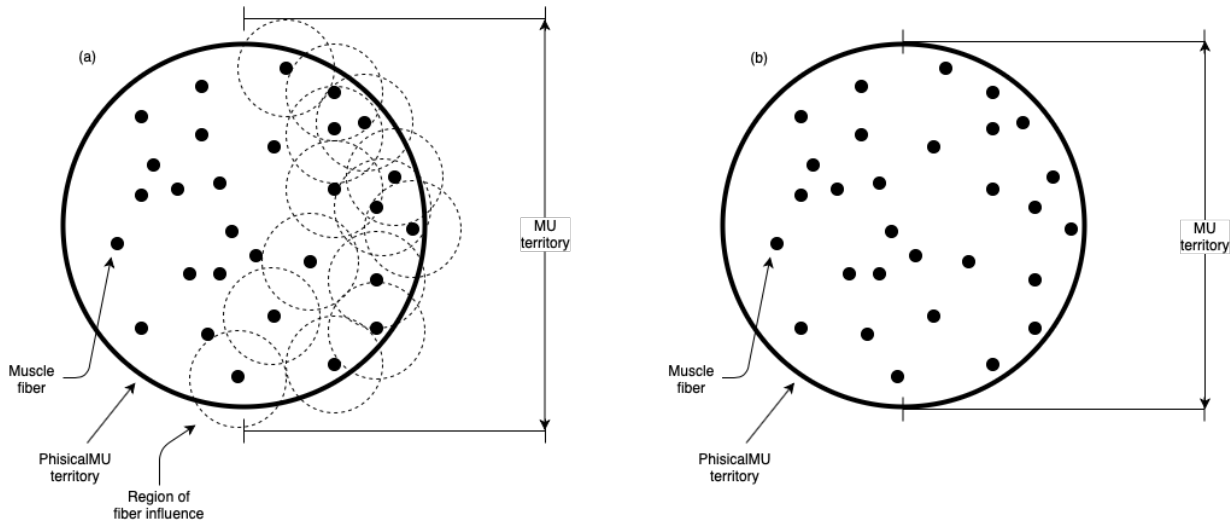


Fig. 7. Estimation of MU territory ground truth limits. (a) Fibers contribution. (b) No fibers contribution.

### 3.1.3 Quality of solutions. Overlapping description.

Each file of solutions, as said, contains a large number of scanning-MUPs having also a variable number of traces thus, they not necessary correspond to MU territories.

A way to determine the overlapping quality of solution on ground truth limits has to be found. This necessity has a further purpose: the only way to know if the proposed algorithms are able to estimate the MUs territory limits is to analyze the results for those signals matched with their reference. At the same time a good degree of overlapping between signals and correspondence ground truth needs to be satisfy. If not, it will be not possible to estimate errors and performing factors.

The manner found to resolve this issue is to implement an algorithm that allows to associate a mark to an investigate solution. Hence, it gives information about the quality of overlapping of the ground truth matching (Fig. 9).

Firstly, the spatial limits in which every multiscanning-MUP is defined are calculated. After that, the marking procedure starts.

For every solution, the initial classification is taken looking at the possibility that the *fibers contribution method*, of ground truth estimation, worked. If so, it is possible to assign three marks to the scanning-MUP under inspection. A mark 0 is given if the spatial location of the signal is completely out from the associated MU territory. In particular, cases of this type can contain only cannula contribution and the detection algorithm must not calculate limits (Fig. 8a). On the other hand, if the solution has some spatial locations in common with the territory the *overlapping coefficient* is



calculated. This number can vary from 0 to 1 and gives information about the percentage of traces that are located inside the territory limits. If this descriptor over the 80% threshold the mark assigned is 2, otherwise it is 1. The meaning of the two grades is relational to the possibility to estimate both the start and the end of a MU territory: a 20% of traces partially or totally inside the correct zone do not provide enough information about the MUP structure, so cases 1 will be discarded for the results comparison. Mark 2 signals are the ones in which all or almost the MU territory is represented and both limits need to be estimates (Fig. 8c)

If the first classification results false, the *no fibers contribution method* is used. If reference limits are available, only mark 0 and 1 can be set. A value of 1 is now related to far MUs contributions with generally small amplitudes so, they will not take into account in the further statistics (Fig. 8b). Instead, marks 0 are set with the same logic previously described.

Finally, if both previous methods fail, the mark is not assigned. These cases will be discarded in next phases, due the impossibility to make comparison between estimations and ground truth.

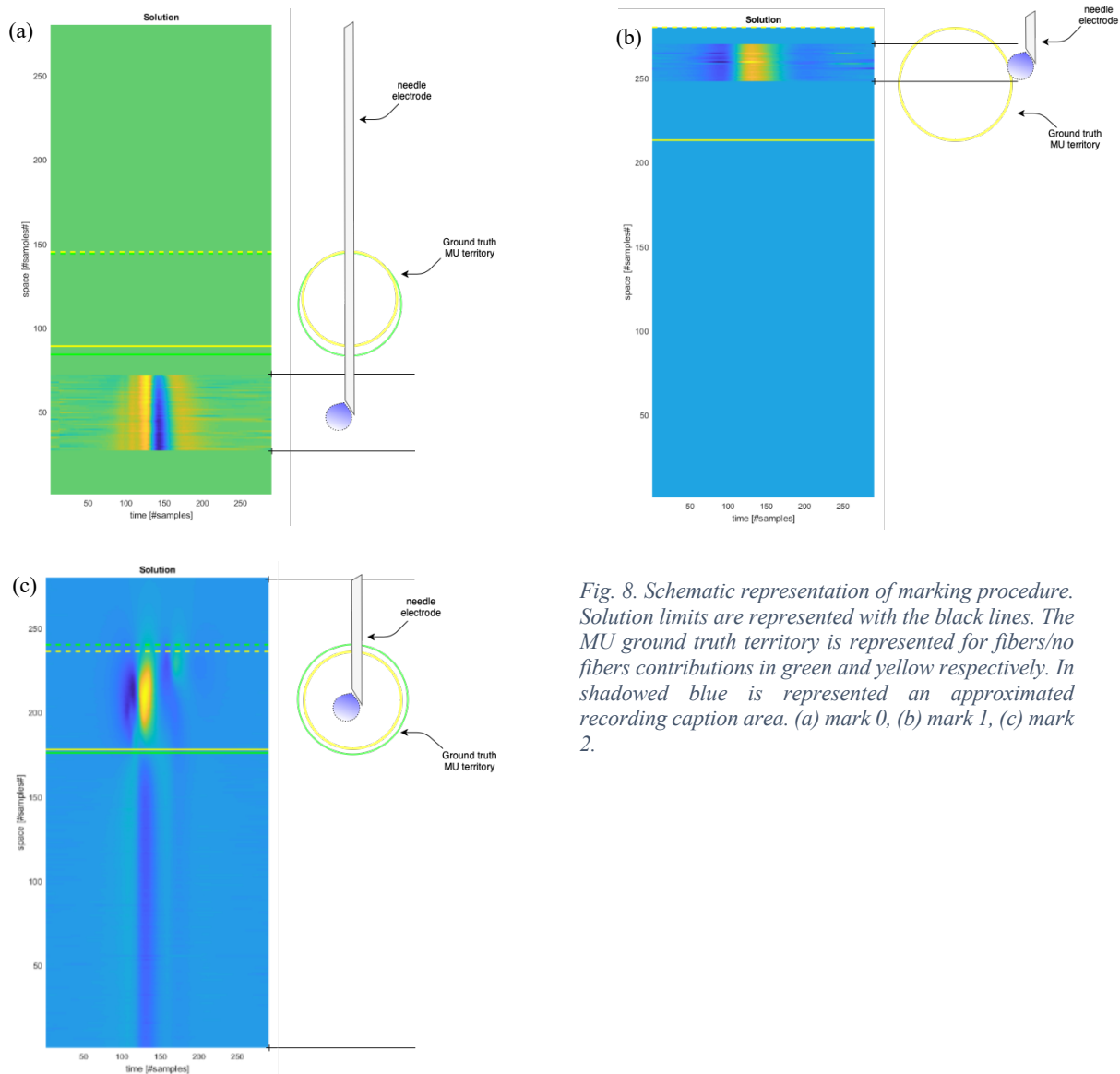


Fig. 8. Schematic representation of marking procedure. Solution limits are represented with the black lines. The MU ground truth territory is represented for fibers/no fibers contributions in green and yellow respectively. In shadowed blue is represented an approximated recording caption area. (a) mark 0, (b) mark 1, (c) mark 2.

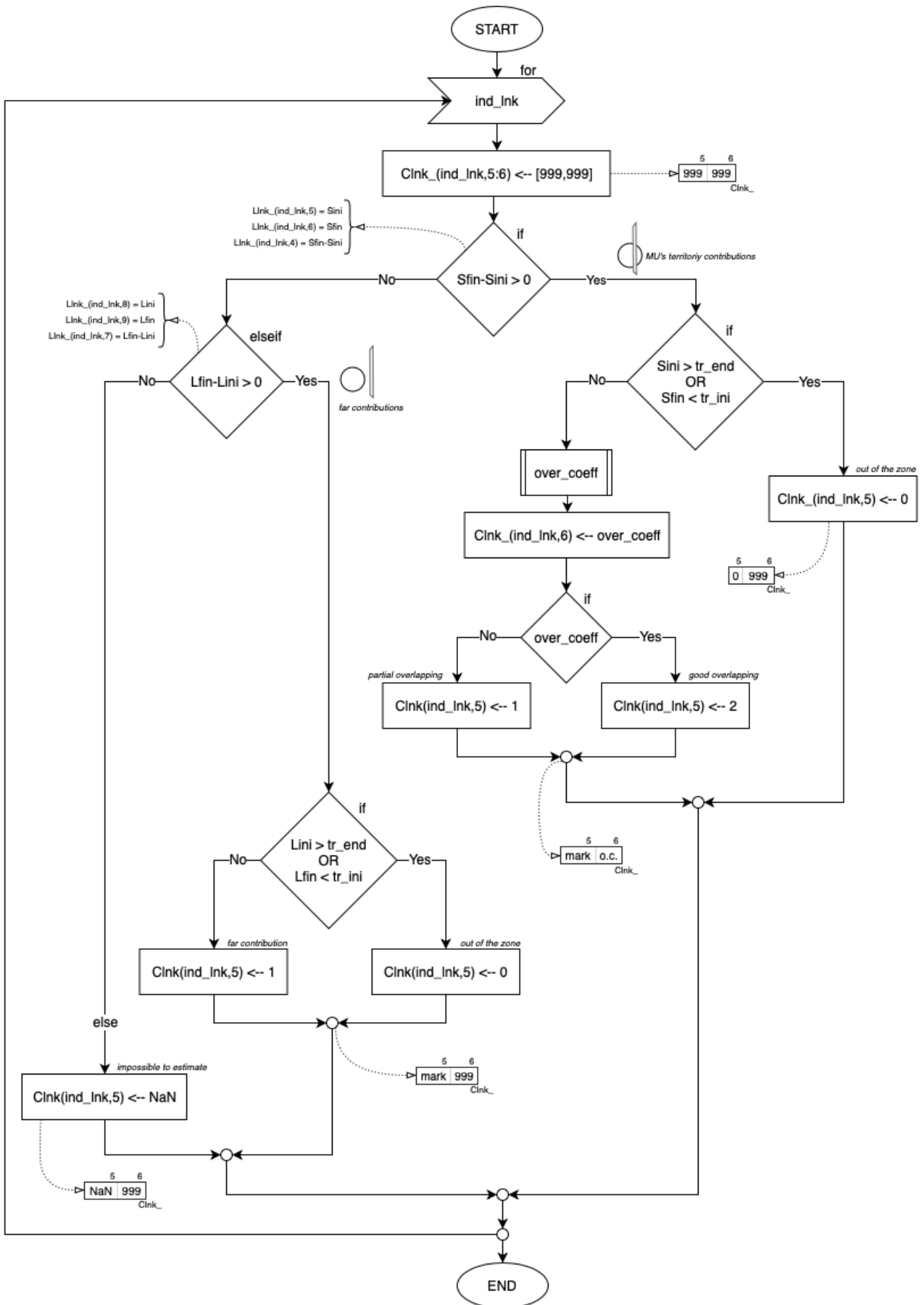


Fig. 9. Scheme of the solutions marking algorithm.

## 3.2 Active region detection algorithms

Three algorithms were implemented and tested in order to estimate the initial and the final limits of the MU territory: *temporal smoothing approach (SA)*, *differential amplitude analysis (DAA)* and *image smoothing method (ISM)*. The first and second are methods based on the knowledge of typical patterns in time duration of the MUs, along all the traces, and in the space-amplitude projection of a scanning-MUP. The third method is based on image processing techniques instead. All of them are implemented via *MatLab* functions and return as output two values corresponding at the spatial locations in which the MU territory starts and end. If the solution does not satisfy certain control criteria, the limits are not calculated, and the returning values are set to 0.

### 3.2.1 Temporal smoothing approach

Amplitude behavior in a MUP can be very variable depending on several factors. From the typical shape of the waveform, the amplitude can vary depending on the distance between MU and electrode, the number of turns can rise depending on the SFAPs timing and finally a pathologic condition can add difficulties to the signal analysis. Time duration behaviors, extracted from a scanning-MUP, produce zones-correlated patterns when they are interpolated along the spatial domain. Hence, the identification and detection of the one related to the MU territory represents the main aim of this algorithm.

#### *Data generation*

From the data matrices stored in every simulation file it is possible to calculate the scanning-MUP duration profiles using the function *scanning\_duration*. The output D matrix has two columns: each row is filled with the initial and final time sample of the MUP detected in that position by the scanning electrode. Hence, the number of rows is equals to the number of spatial samples of the solution.

The method of calculation of these limits is done with a threshold based on the maximum peak, that can be relative to every trace or absolute, looking at the whole scanning-MUP data matrix. In this case, the relative calculation is selected in order to obtain the waveforms useful to the further analysis: in correspondence of the MU territory, initial and ending duration points show, in a first analysis, symmetric parabolic behaviors through the spatial dimension. In the cannula zone, the durations have an almost linear behavior and are more spread around this regressor (Fig. 11).

Finally, rows of D can contain or positive integer numbers (duration limits as said) or not calculating values, depending on which spatial position a solution trace is stored. The later occurs when a scanning-MUP row does not present an available trace in that specific spatial position.

# The algorithm

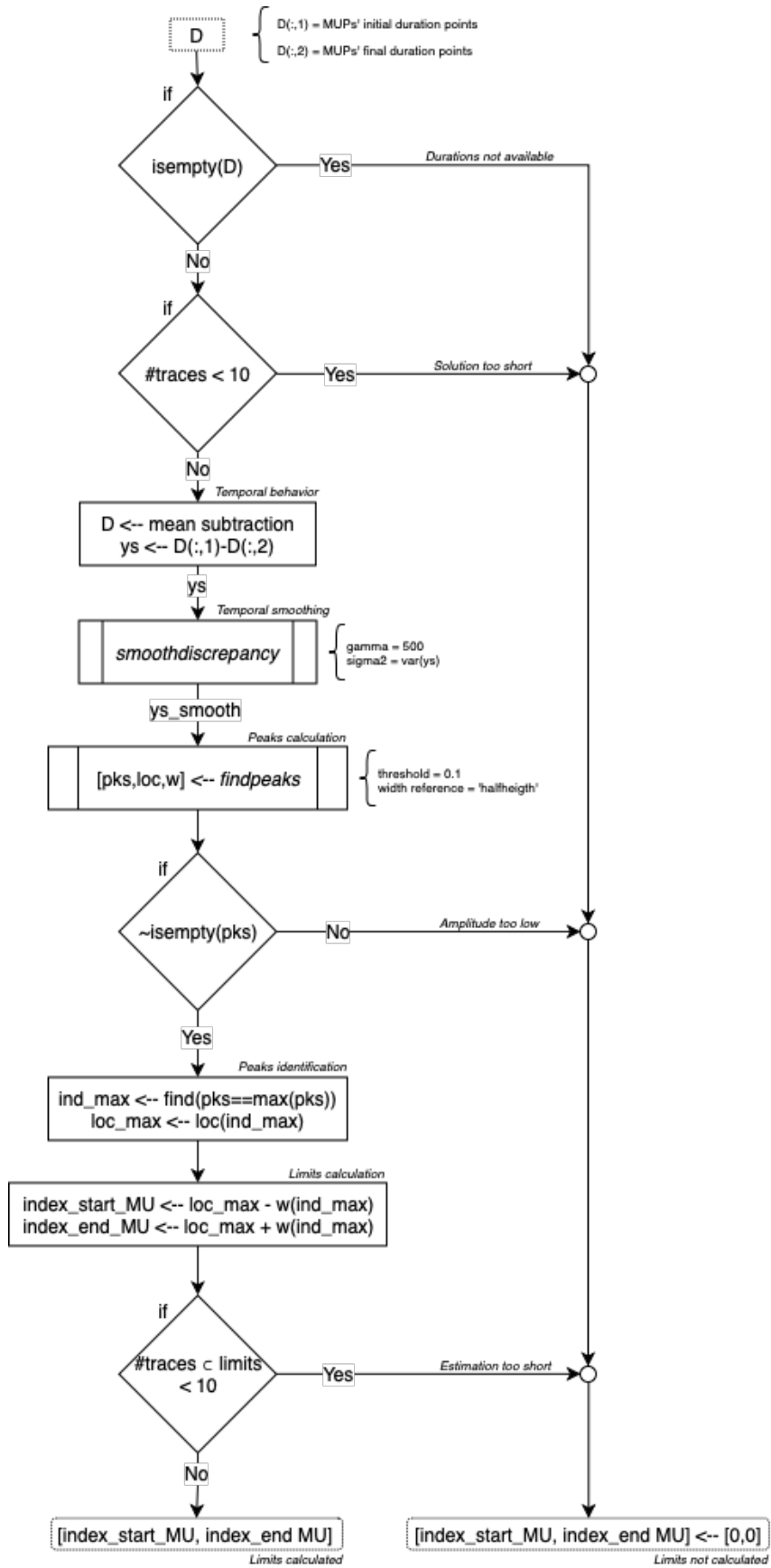


Fig. 10. Scheme of TSA algorithm.

Once the matrix D matrix is created, it can be passed as input to the function *smoothed\_approach\_fun* that implements the algorithm under investigation (Fig. 10).

The first phase consists on preprocessing the data directly classifying as not having an active region any record in which D is empty or the number of traces of the solution is below 10.

If the signal is not purged by this first classification, the correct portion of data is selected, baseline subtraction is performed for each column and a definitive signal is created subtracting each other the initial and the ending duration points. This final procedure is done in order to improve the detection of the particular MU-related parabolic pattern. In fact, its amplitude is emphasized, respect to cannula contributions, if this subtraction is performed (Fig. 11).

After the data preprocessing, the algorithm starts with MU territory detection. As said, the goal is to improve the characteristic peaks behavior in this region of interest. However, the latest subtraction increases the ripple of the resulting signal, so an additional filter is necessary. The method used to solve this issue consists on finding a smoothed curve that interpolates data using the function *smoothdiscrepancy*, that performs a WLLS smoothing controlled by the parameter *gamma*, set as 500. The result is a low pass filtered version of the original signal. Then, the MatLab function *findpeaks* is used to detect the highest peak, its location and its width depending also on a threshold set at 0.1. Doing this, the center location of the MU territory is found and limits are taken summing and subtracting at this the peak width.

Ulterior controls are inserted to discard that estimations that, at the end of the process, have a number of traces below 10, in accordance to the preprocessing.

### Example of operation

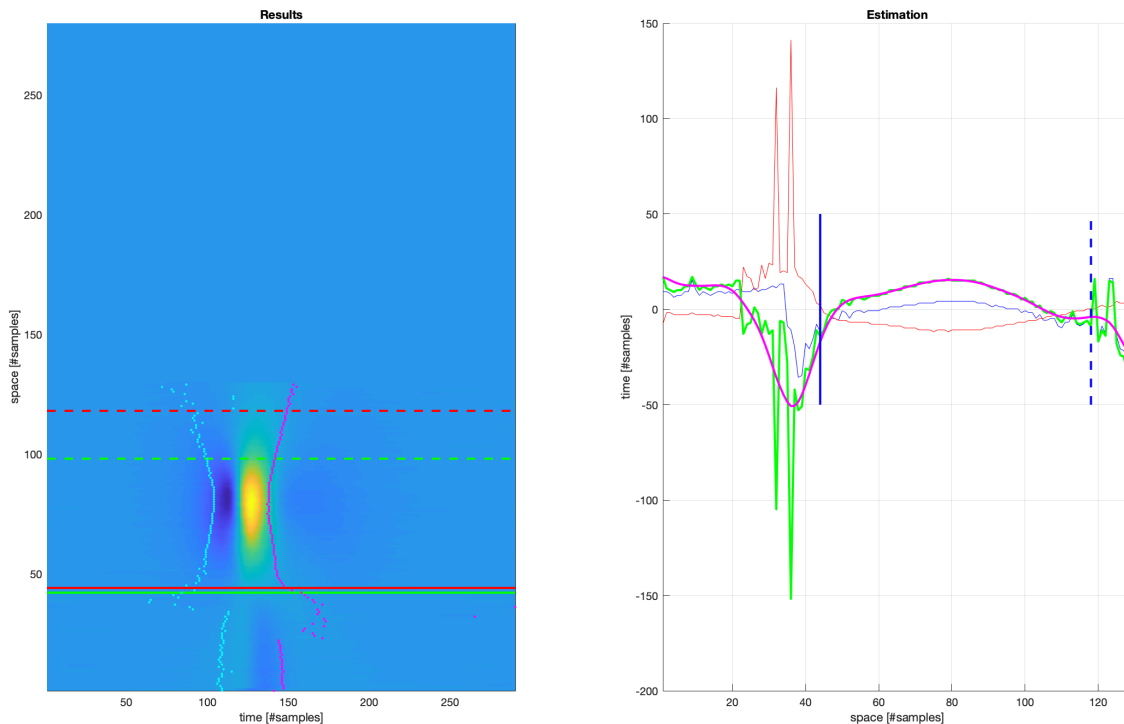


Fig. 11. TSA estimation. On the right: duration data (blue and red), their subtraction (green), smoothing (magenta) and limits (blue). On the left: solution with durations data (cyan and magenta), ground truth (green) and estimation (red).

### 3.2.2 Differential amplitude analysis

The results obtained with the previous method show a certain under- and over-estimation in the detection of initial and ending points respectively. The scanning-MUP amplitude has to be used to improve the performance. In this second proposal, the data of the amplitude-spatial projections are used to estimate limits. After the calculation of the first derivate of these behaviors a peaks selection is performed: MU territory will be included between the higher and lower spatial position in which the highest peaks occur.

#### *Data generation*

The function *scanning\_profile* returns on output a variable in which space-amplitude and space-temporal 2D turns projections, of the original scanning-MUP, are calculated.

The algorithm of MUP's profile extraction, as seen in section 2.3, can link turns along spatial dimension with a point tracking algorithm. When a line of points is found it is saved in a row of the corresponding projection matrices, temporal and amplitude, of the same sign and on the correct scanning location. Once the procedure is finished, the matrices have a number of rows equal to the turns profile linked and this number can be different between negative and positive trajectories.

#### *The algorithm*

After several improvements of the algorithm it was possible to notice that positive amplitude projections provide a set of signals with higher slope in MU territories and longer traces than the negative ones. So, only these behaviors were selected for the further analysis.

In the preprocessing phase, two types of escape controls are implemented: first of all, limits are not calculated if the profile loaded is empty; and second, the algorithm stops if the number of valid MUP traces is below 10.

Ensuring that the loaded profile can be processed, for each row of the data matrix the first derivate is calculated and a gaussian filter, with a standard deviation of 1.6 and a length of 9 samples, is subsequently applied. The filter is needed to smooth the output signal of the previous calculation because of an increment of the ripple of the curve after the first derivative is calculated.

The main part of the code consists on the peaks detection on the derivative-filtered signals created before. As said, the highest slopes contribution on the highest amplitude projection give information about the start and the end of the MU territory. So, peaks are detected, using the function *findpeaks*, on the rectified version of the just calculated differential data matrix, only if they take values over a threshold fixed at 0.25mV/space sample. This first preselection makes possible to discard almost every cannula contribution because in this zone the amplitude signals are almost constant, hence the derivative components are null. Also, the threshold cannot be set too low, or the next calculations can be inaccurate. Once peaks, their locations and their half-height widths are detected, looking at all the traces in the data matrix, the limits estimation is performed: the start of the territory is taken as the deepest location at which is subtracted the half-width of its corresponding peak and the end of the territory is taken as the most superficial location.

Further controls are finally implemented. If the peaks are not found or if the number of traces between the estimate limits are below 10 than the return values are set to 0.

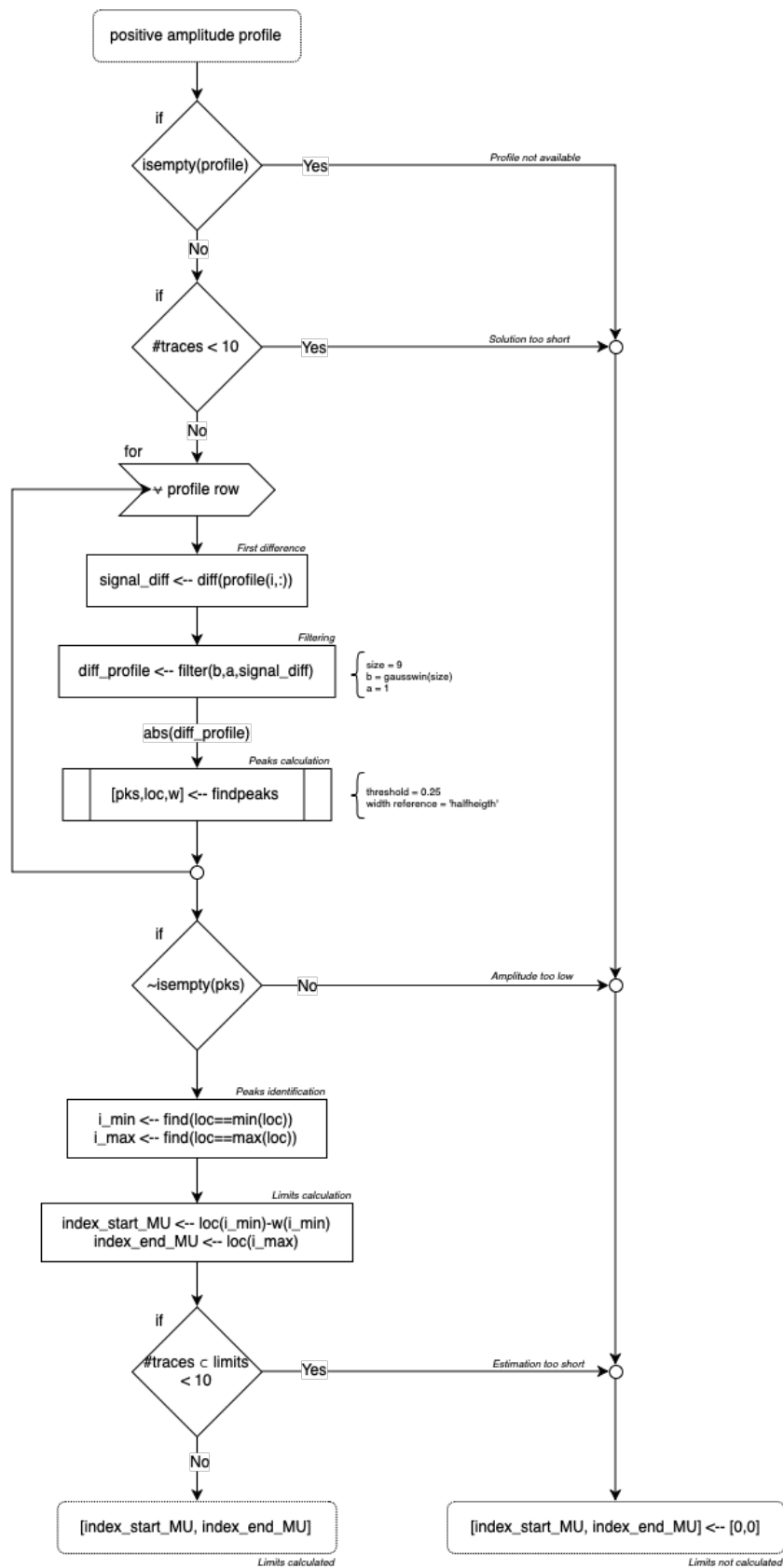


Fig. 12. Scheme of DAA algorithm.

### Example of operation

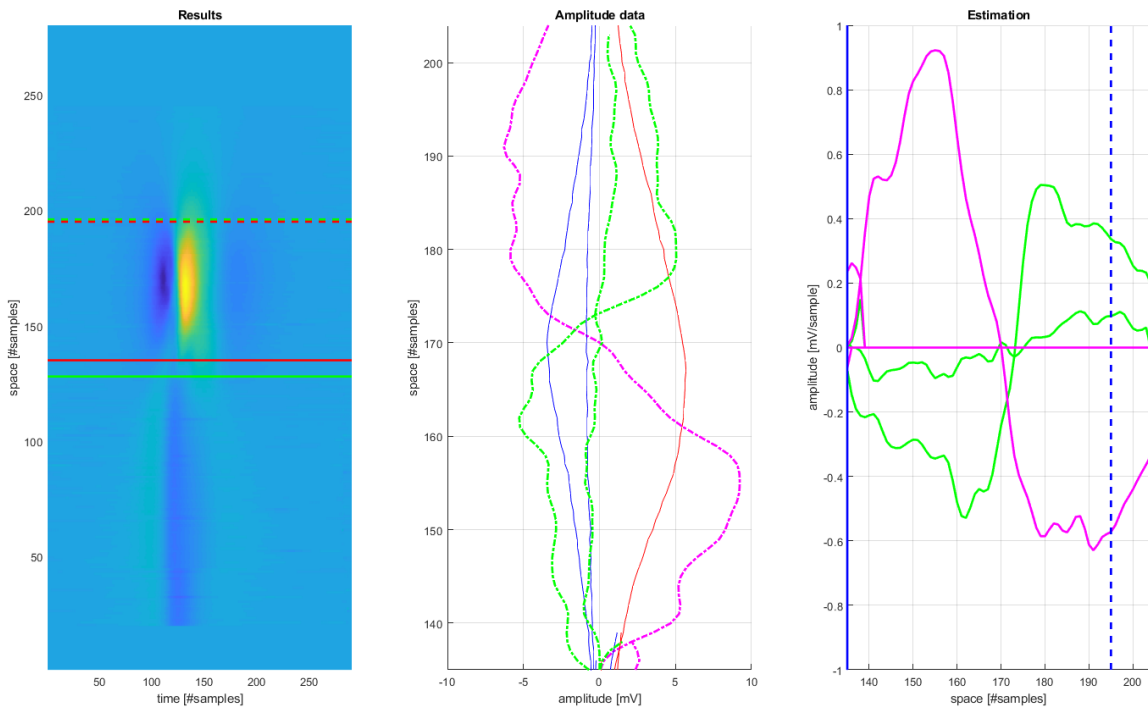


Fig. 13. DAA estimation. Amplitude profile data (blue and red), their derivative components (green and magenta).

### 3.2.3 Image segmentation method

Scanning-MUP signals can be represented as images. It is easy to see that a MU territory is clearly represented in a color-map, as reported in chapter 2.2. In this method, we propose to use a contour segmentation in order to detect this characteristic zone.

#### *Data generation*

Data are just represented by the scanning-MUP matrices. No data processing is needed.

#### *The algorithm*

The scanning-MUP data matrix is preprocessed in order to discard it if its number of valid traces, so not zero rows, is below 10 or if its maximal amplitude is below the 1mV threshold. This last control is imposed from the scanning-MUP observation: MUs detected in proximity of the scanning electrode have peaks' amplitudes that easily overtake this imposition, so far contributions, probably MUs not traversed by the scanning corridor, are discarded. Also, images that represent only cannula zone can be neglected too.

Data can be affected by noise and there can be large changes in amplitude between nearby cells, or pixels. Hence, as in the previous methods a filtering process is performed. In this case the function *imgaussfilt* allows to smooth an image in both dimension with a gaussian kernel with size 5, wide of



a square of nearby cells, and standard deviation equals to 3. The result has an improved uniformity of amplitudes, although some of the definition of the image is lost.

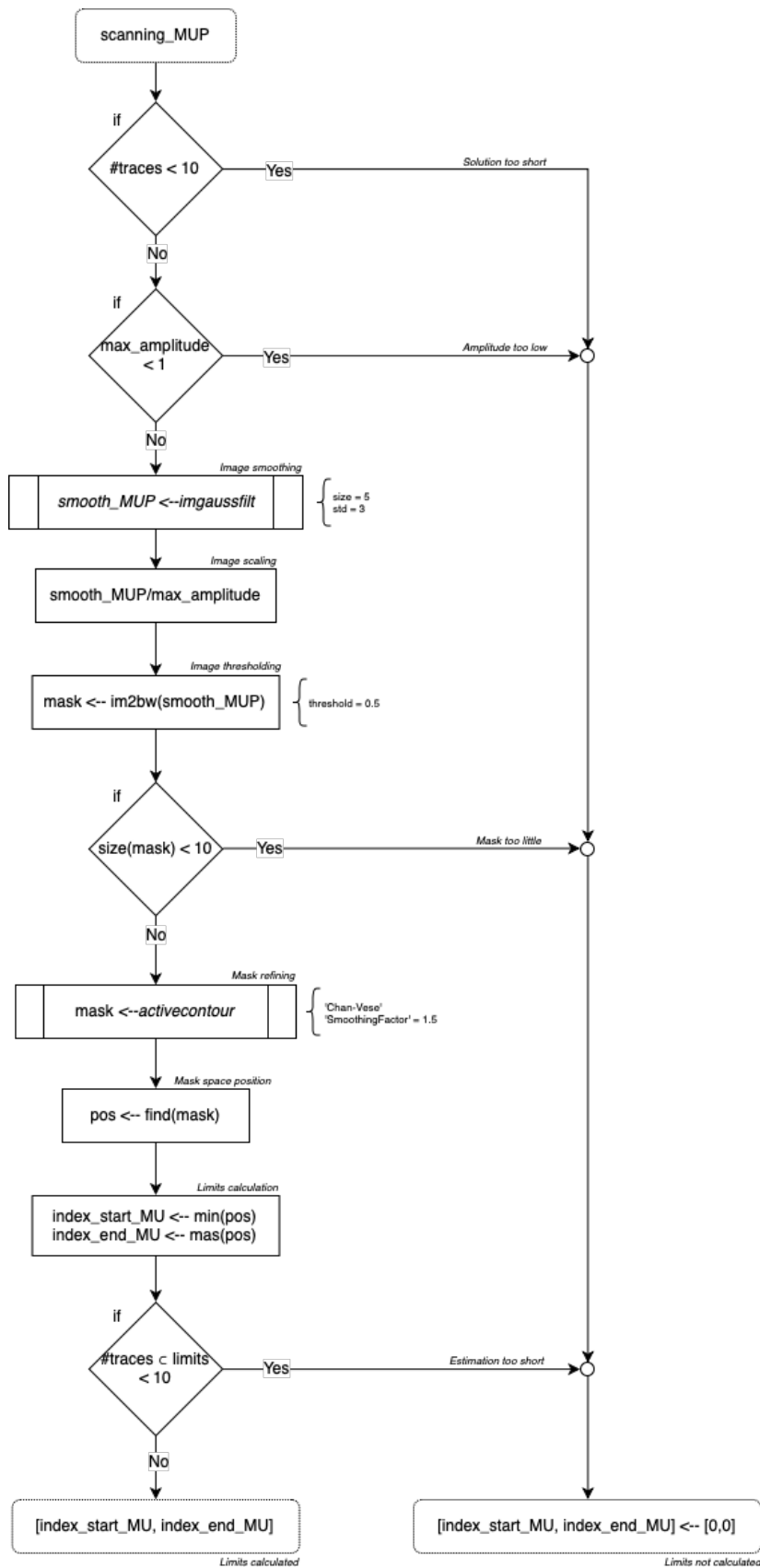


Fig. 14. Scheme of ISM algorithm.

The next phase consists on defining a preliminary mask that can segment the positive hill, or more than one, that represent the MU territory. Firstly, the image is scaled in the interval  $[-1,1]$  dividing it by its maximum value found during the preprocessing. A thresholding is next applied selecting all the amplitude values that are over a 50% of the maximum peak. The mask obtained is a raw version of the segmentation, but it can be possible to perform already a first type of control: if the number of 1-pixels is below 10 the algorithm stops and classify the signal as not having an active MUP region. This approach wants to avoid the possibility that the resulting mask is empty and, in particular, wants to discard the limit case in which it is composed by a set of aligned pixels in the spatial dimension. If the result respects these limits the mask is refined, and its contours smoothed. The *activecontour* function accomplishes these tasks selecting as input parameters *Chan-Vese*, as force calculation method, and a smoothing factor of 1.5. The achieved mask now overlaps the MU territory taking as limits the points in which the slope of the positive hill satisfies the desired gradient conditions [10].

Latest step is the limits estimation accomplished selecting the deepest and de most superficial spatial coordinates of the mask. A last control is made discarding the solution if the number of traces between the limits is below 10.

### Example of operation

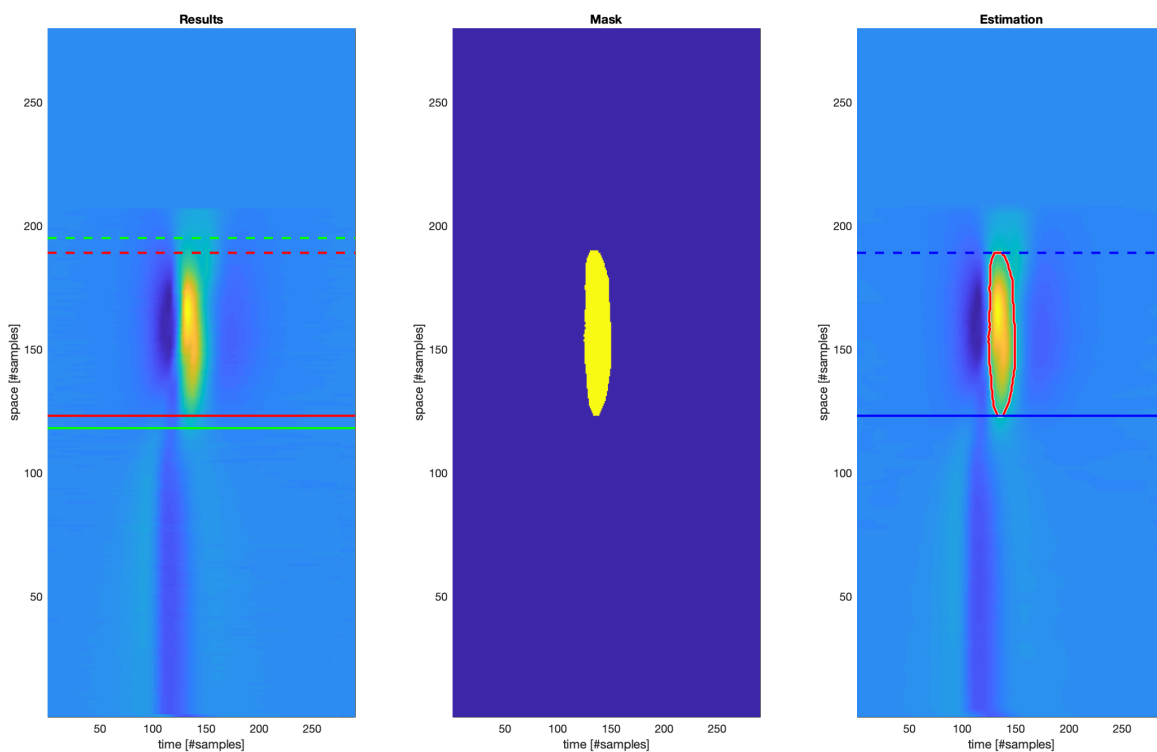


Fig. 15. ISM estimation.

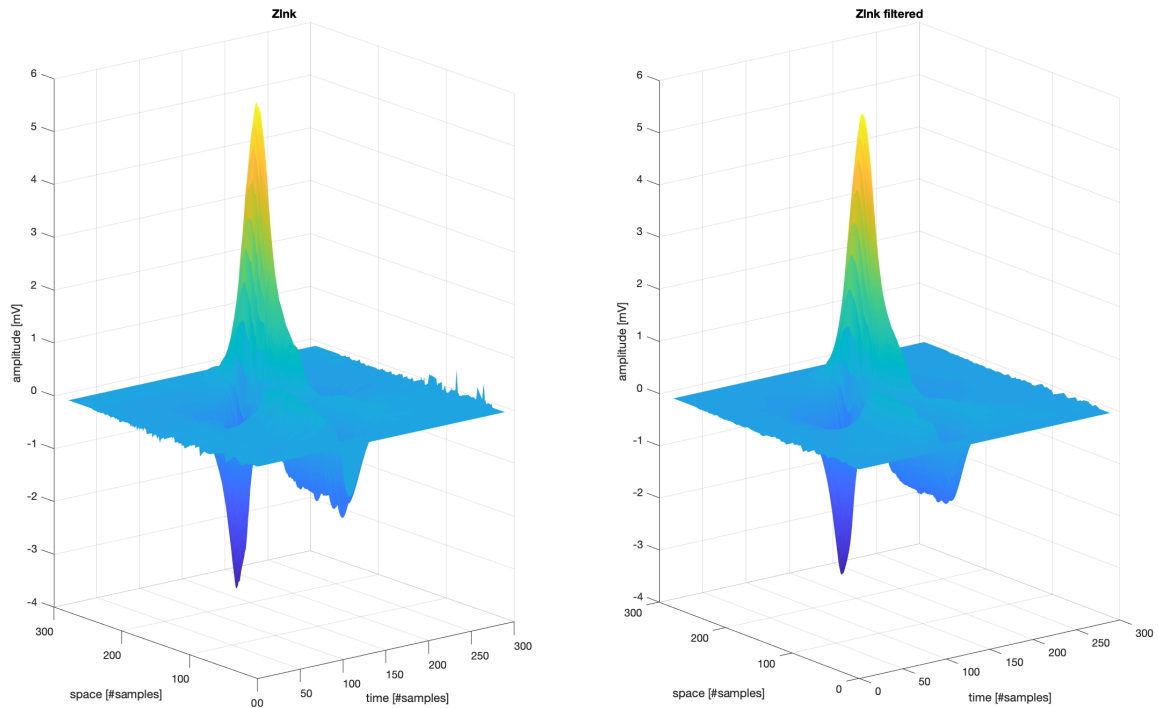


Fig. 16. Effect of the 2D filter. On the right is reported the filtered version of the solution on the left.

### 3.3 Auxiliary functions and scripts

#### 3.3.1 Error finder

The database under inspection contains a large number of solutions divided in a large number of files too. After processing the results and ground truth of every folder, data are concatenated in their corresponding matrix acquiring new ‘global’ indices. So, the original relative position of every record within global results must to be calculated.

The function *error\_finder* accomplishes this task by processing the acquired database information. The output linking is given as a structured variable where each row reports the name of the file, its identifier number and the relative index of the scanning-MUP solutions to be inspected. Changing the value of a flag input variable it is also possible reconstruct the original position of a single solution.

#### 3.3.2 Trace inspectors

The estimation algorithms are implemented in MatLab functions. They have to be performant and easy to understand so the graphical content is not necessary. But when an error occurs, the best way to know why a method fails is to have a look to a graphical description of it.

Three functions, one for each algorithm, can be used in combination with *error\_finder* to show how the limits are calculated. Also, ground truth limits are linked and plotted in order to have a complete characterization of the investigated solution.

These functions were used to create the example figures reported in the previous sub-chapters.



## 4 Final results and discussion

In this chapter individual results and comparison between methods are analyzed. The data marking presented in 3.1 also allows to discard those signals not representing significative MU territories, so those not linked with a reference or with a low number of traces. Hence, the estimation of the errors is provided by looking only for that solutions well overlapped with the ground truth. The classification of the simulation-linked signals but with spatial locations outside the reference limits it is another performance parameter to take into account. Also, individual results can be studied according to their MVCs. Finally, comparisons between the three methods are presented.

### 4.1 Results of individual methods

Individual results are estimated according on the MVCs and the matrix of scanning-MUP marks. Selecting the results as a function of the MVC is interesting in order to know if the algorithms, with an increment of recruited MUs, depend on the noise produced in the solutions. In the second case the mark 2 selection (scanning-MUP solutions where MU limits can be estimated) allows to characterize and refine the estimation errors.

According to a specific MVC selection, the database can be divided as reported in Tab. 2.

<i>Number of</i>	<i>All MVCs</i>	<i>MVC 2%</i>	<i>MVC 3%</i>	<i>MVC 4%</i>
<b><i>Solutions</i></b>	14368	3094	4948	6326
<b><i>Solution discarded</i></b>	10972 (76.23%)	2022 (65.35%)	3795 (76.70%)	5155 (81.49%)
<b><i>Solutions analyzed</i></b>	3396 (23.64%)	1072 (34.65%)	1153 (23.30%)	1171 (18.51%)
<b><i>Mark 0</i></b>	274 (8.07%)	202 (18.84%)	51 (4.42%)	21 (1.79%)
<b><i>Mark 1</i></b>	1769 (52.09%)	562 (52.43%)	608 (52.73%)	599 (51.15%)
<b><i>Mark 2</i></b>	1353 (39.84%)	308 (28.73%)	494 (42.84%)	551 (47.05%)

Tab. 2. Composition of the database.

A first selection is performed in order to discard that solutions not linked with a simulated MUP. In these, a correspondence with the ground truth was not found, so results cannot be compared with reference values. Less of a quarter of the total number of solutions are processed and of this another partition can be found according with marks. The *mark 1* ones represent those data not well overlapped with true limits or those in which MUs' far contributions are recorded. These are also discarded in next phases. *Mark 0* and *mark 2* solutions are the ones in which the estimation algorithms must to work and detect limits, where necessary, in the correct manner. Hence, only the 48% of the scans analyzed are used for the evaluation of the algorithms, less than the 10% of the total database.

In the next sections, results are presented graphically for each method and a final discussion is reported in 4.1.4. Several merit figures will be analyzed:

- *Confusion matrix*: reports the number of true negatives, false positives, true positives and false negatives. The first two are taken for mark 0 cases, the other for mark 2 cases. In particular, true negative is determined when the algorithm detects a signal not useful, instead a true positive is determined when a MU is detected, and the limits calculation can be performed.
- *Error distribution*: only for cases 2, allows to show characteristics of under/over estimation and statistic indices can be calculated.
- *Relative error vs length of solution*: only for cases 2, shows the relationship between errors and length of the solutions analyzed. Relative error is taken as ration between absolute error and ground truth.
- *Error vs MVC*: only for cases 2, shows the relationship between MVC and errors.

The main goal of the algorithms is to estimate the initial and final limits of the MUs detected. So, figures report both the estimation errors.

### 4.1.1 Temporal smoothing approach

#### Confusion matrix

		<i>Estimation</i>		
		Not calculated	Calculated	False rate
<i>Truth</i>	Out of territory	259	15	5.47%
	Inside of territory	25	1328	1.85%

Tab. 3. TSA confusion matrix.

#### Error distribution

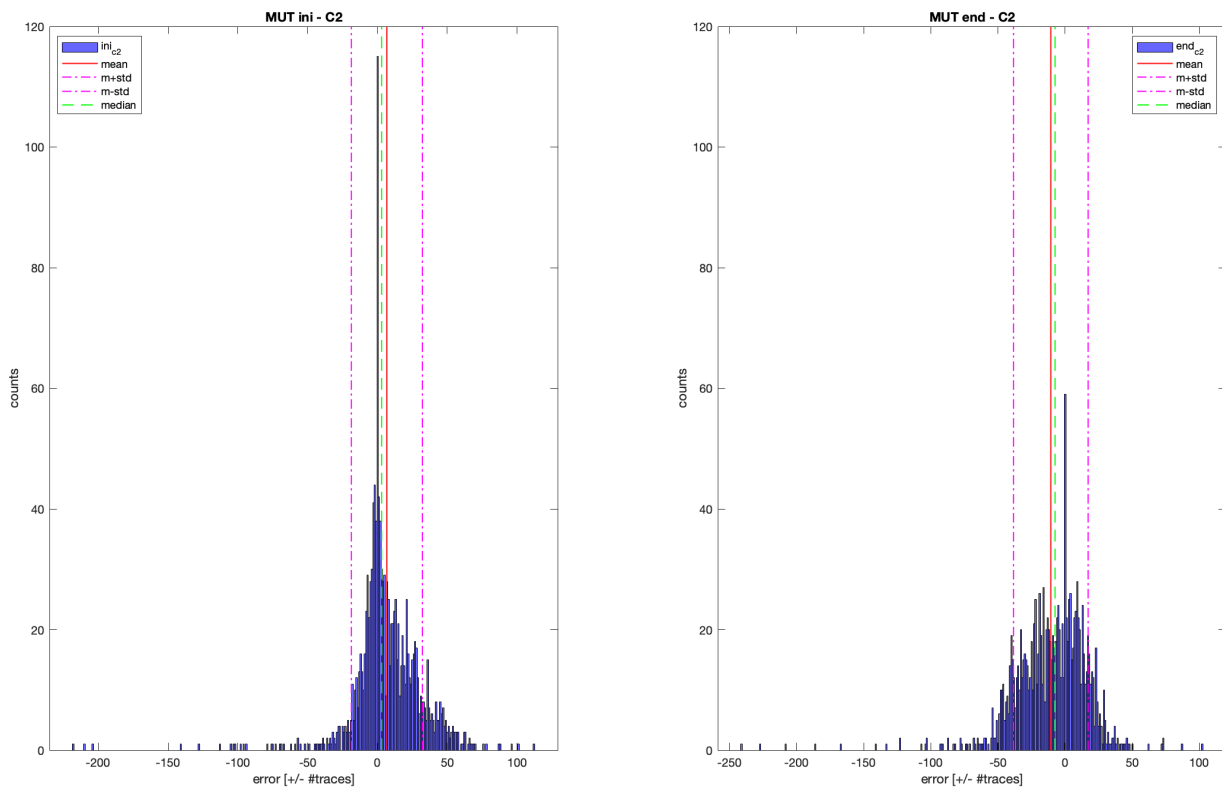


Fig. 17. TSA error distribution.

<i>Statistical data [# traces]</i>					
	Mean	Standard deviation	Median	25 <sup>th</sup> percentile	75 <sup>th</sup> percentile
<i>Initial limit</i>	6.6943	25.4368	3	-3	20
<i>Final limit</i>	-10.6852	27.7836	-7.5	-26	7

Tab. 4. TSA error distribution, statistical data.

### Relative error vs length of solution

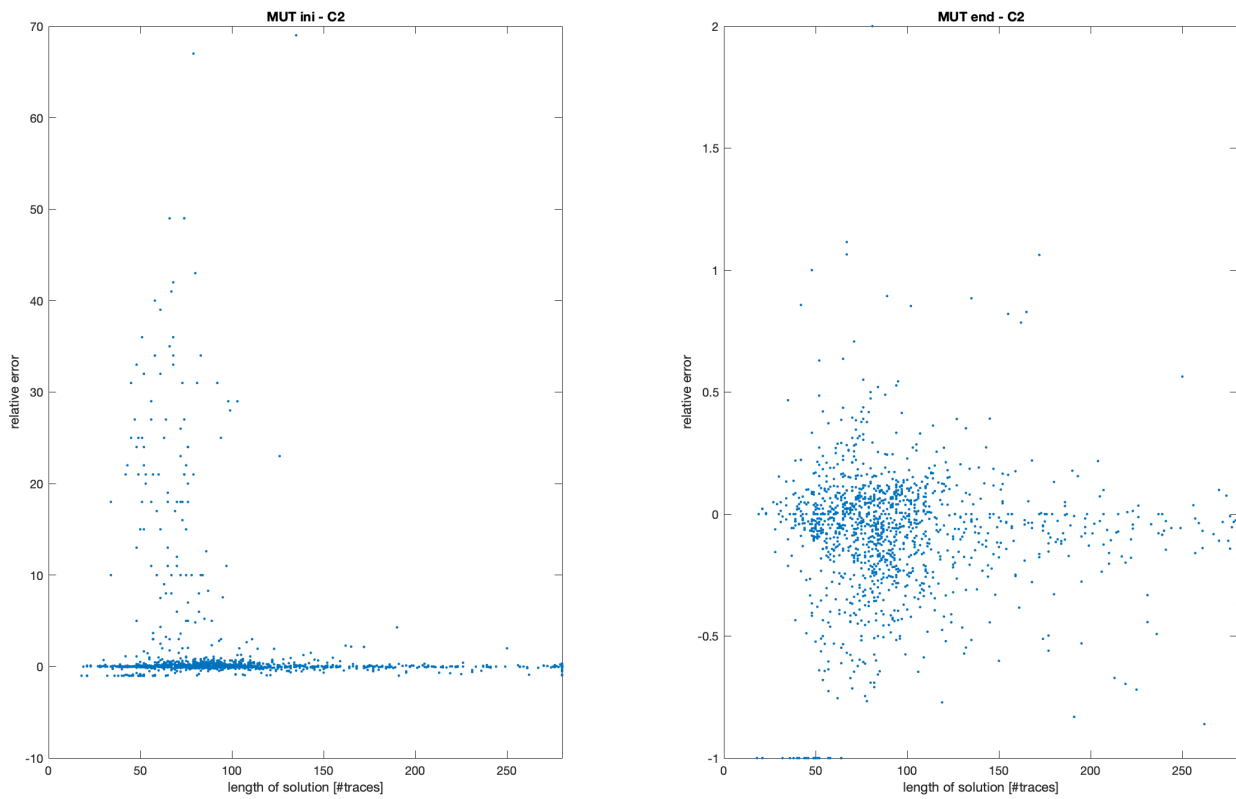


Fig. 18. TSA relative error vs length of the solution.

### Error vs MVC

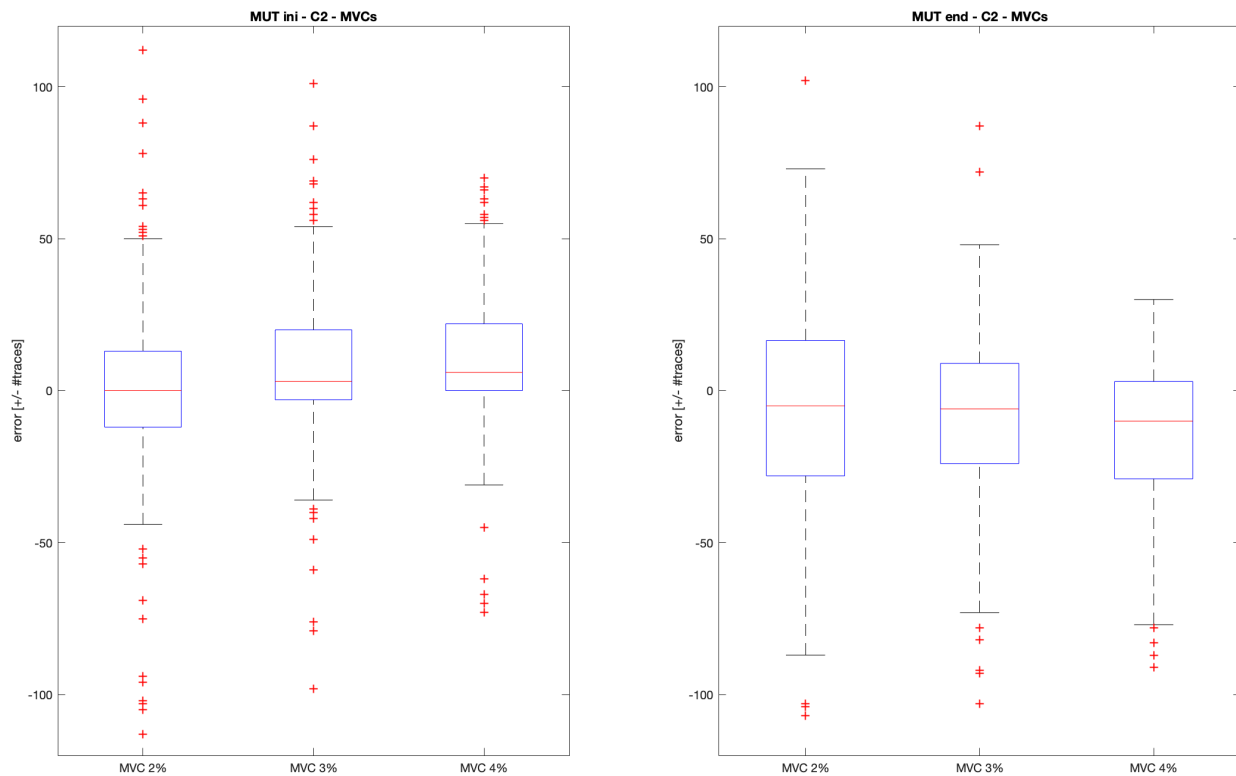


Fig. 19. TSA error distribution error vs MVCs.



		<i>Statistical data [# traces]</i>		
		<b>Median</b>	<b>25<sup>th</sup> percentile</b>	<b>75<sup>th</sup> percentile</b>
<b><i>Initial limit</i></b>	MVC 2%	0	-12	13
	MVC 3%	3	-3	20
	MVC 4%	6	0	22
<b><i>Final limit</i></b>	MVC 2%	-5	-28	16.5
	MVC 3%	-6	-24	9
	MVC 4%	-10	-29	3

*Tab. 5. TSA error distribution vs MVCs, statistical data*

## 4.1.2 Differential amplitude analysis

### Confusion matrix

		<i>Estimation</i>		
		Not calculated	Calculated	False rate
<i>Truth</i>	Out of territory	274	0	0.00%
	Inside of territory	52	1301	3.84%

Tab. 6. DAA confusion matrix.

### Error distribution

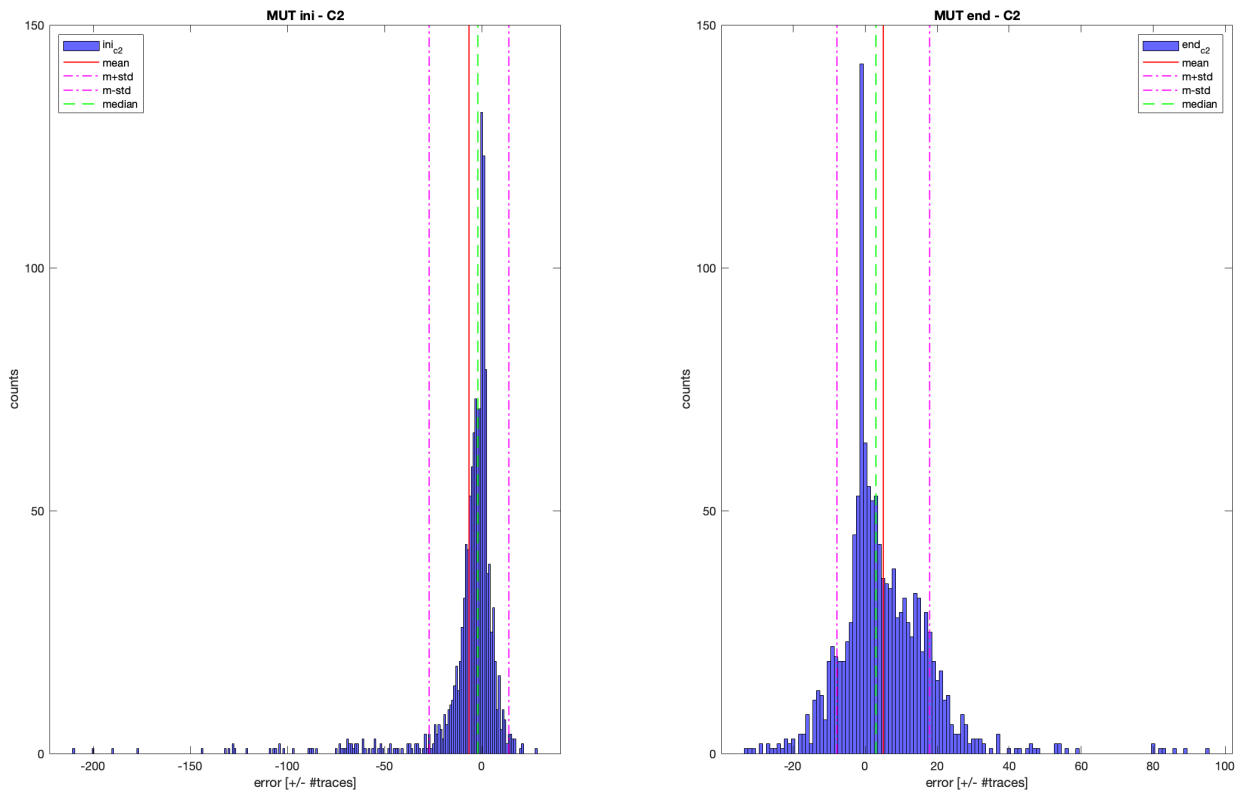


Fig. 20. DAA error distribution.

<i>Statistical data [# traces]</i>					
	Mean	Standard deviation	Median	25 <sup>th</sup> percentile	75 <sup>th</sup> percentile
<i>Initial limit</i>	-6.5719	20.5127	-2	-7	1
<i>Final limit</i>	5.0477	12.8675	3	-2	12

Tab. 7. DAA error distribution, statistical data.

### Relative error vs length of solution

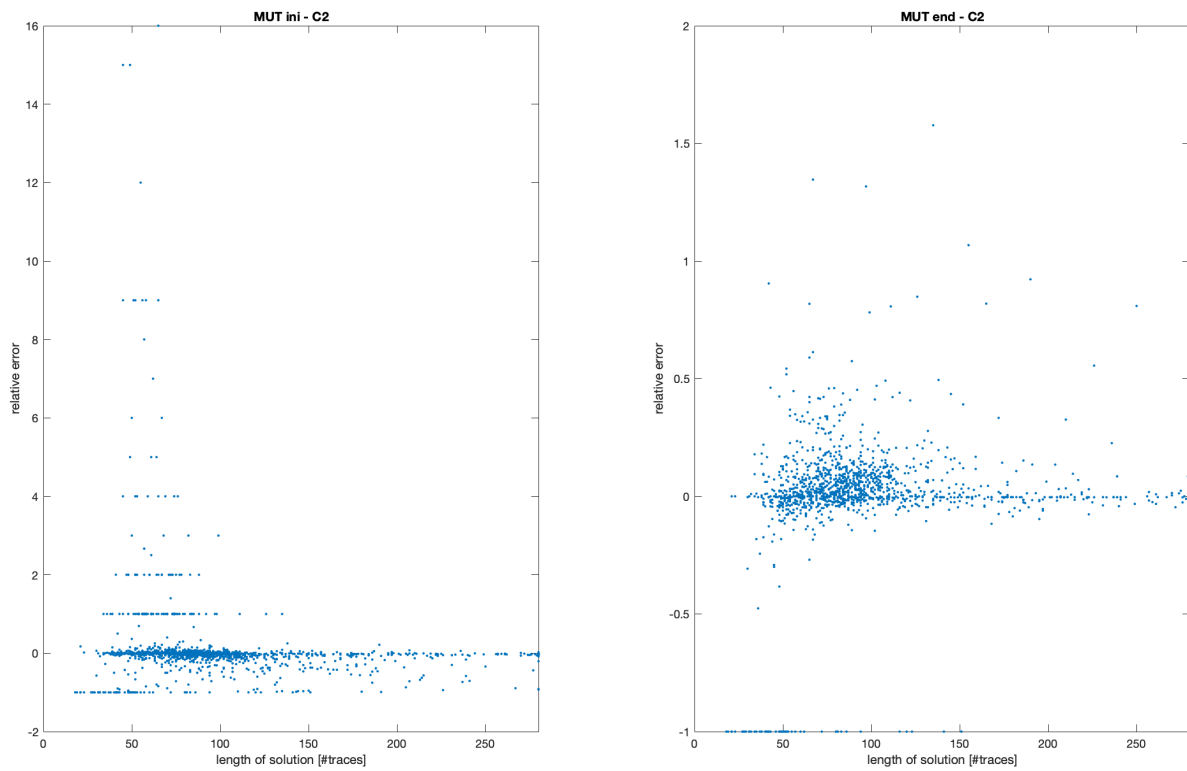


Fig. 21. DAA relative error vs length of the solution.

### Error vs MVC

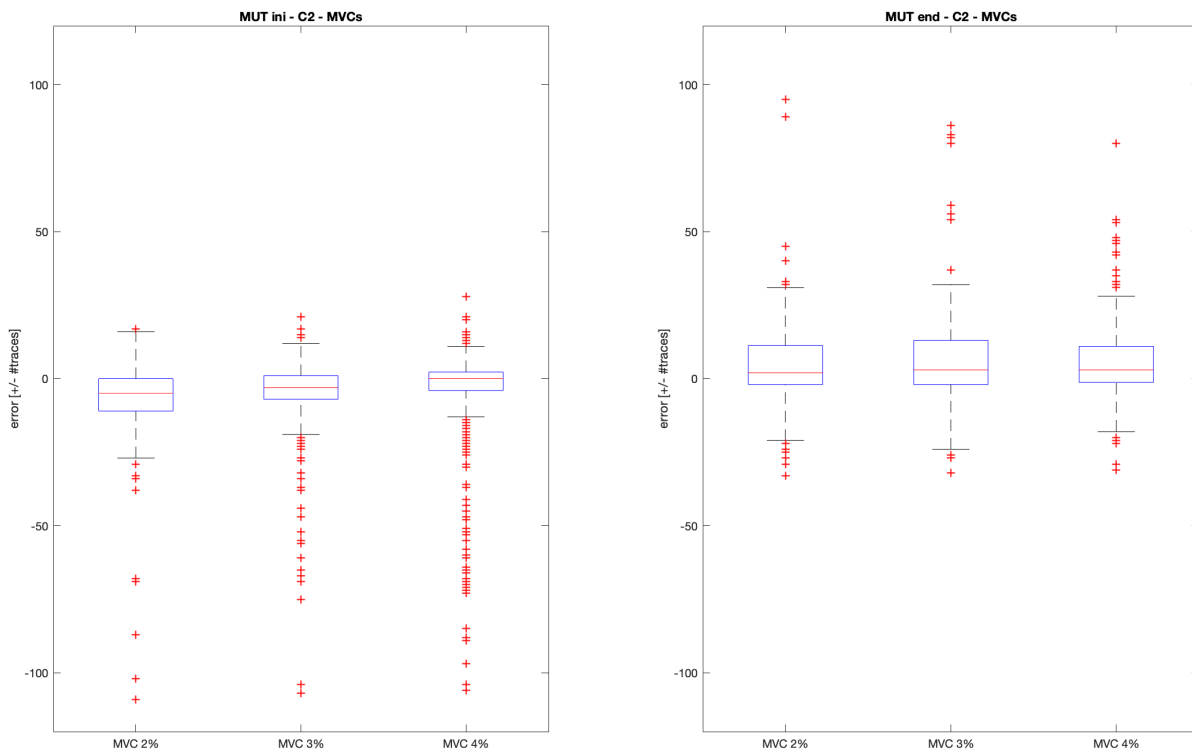


Fig. 22. DAA error distribution vs MVCs.

		<i>Statistical data [# traces]</i>		
		<b>Median</b>	<b>25<sup>th</sup> percentile</b>	<b>75<sup>th</sup> percentile</b>
<b><i>Initial limit</i></b>	MVC 2%	-5	-11	0
	MVC 3%	-3	-7	1
	MVC 4%	0	-4	2.25
<b><i>Final limit</i></b>	MVC 2%	2	-2	11.25
	MVC 3%	3	-2	13
	MVC 4%	3	-1.25	11

*Tab. 8. DAA error distribution vs MVCs, statistical data.*

### 4.1.3 Image segmentation method

#### Confusion matrix

		<i>Estimation</i>		
		Not calculated	Calculated	False rate
<i>Truth</i>	Out of territory	274	0	0.00%
	Inside of territory	18	1335	1.33%

Tab. 9. ISM confusion matrix.

#### Error distribution

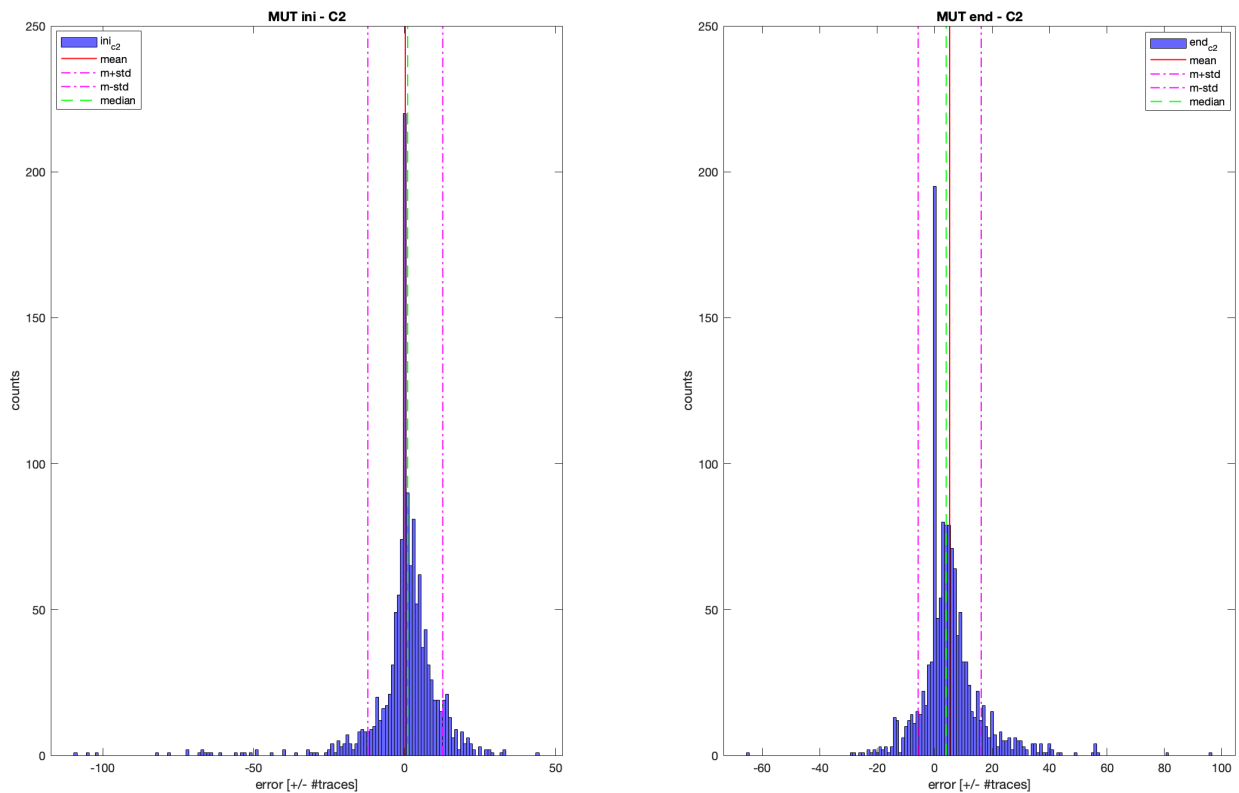


Fig. 23. ISM error distribution.

<i>Statistical data [# traces]</i>					
	Mean	Standard deviation	Median	25 <sup>th</sup> percentile	75 <sup>th</sup> percentile
<i>Initial limit</i>	-0.2150	12.7105	0	-2	5
<i>Final limit</i>	5.6509	11.4027	4	0	9

Tab. 10. ISM error distribution, statistical data

### Relative error vs length of solution

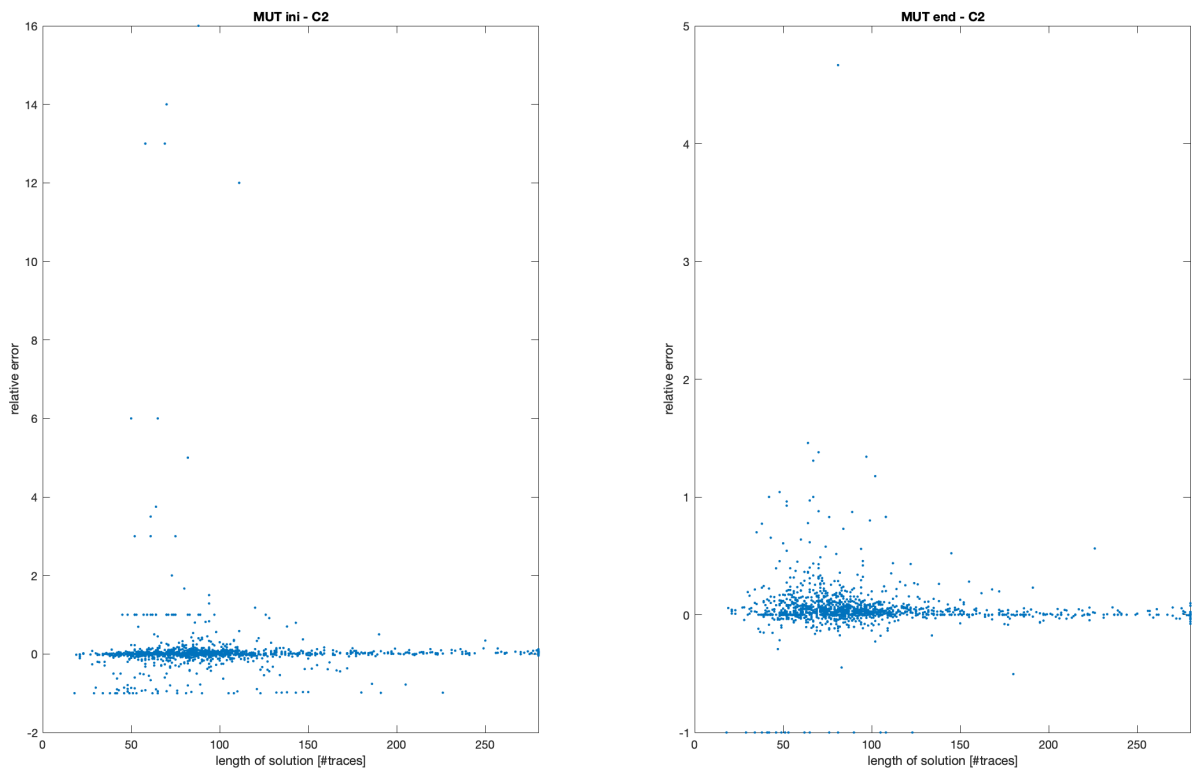


Fig. 24. ISM relative error vs length of the solution.

### Error vs MVC

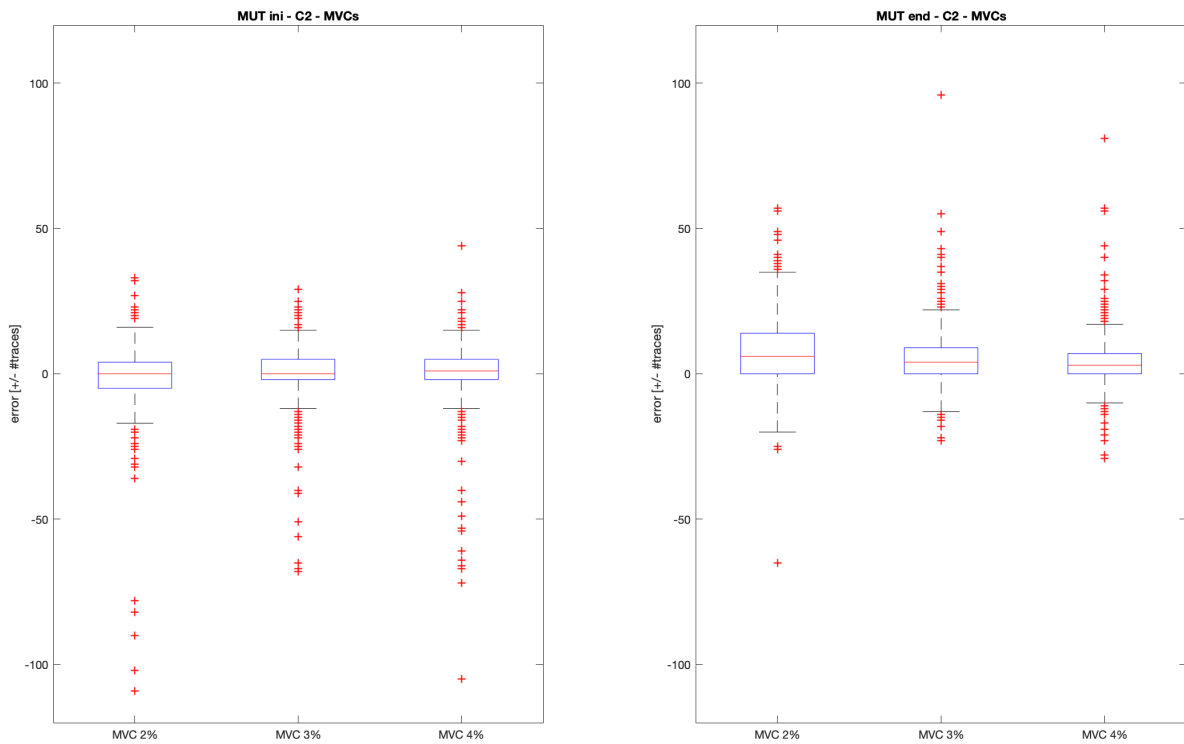


Fig. 25. ISM error distribution vs MVCs.

		<i>Statistical data [# traces]</i>		
		Median	25 <sup>th</sup> percentile	75 <sup>th</sup> percentile
<b>Initial limit</b>	MVC 2%	0	-5	4
	MVC 3%	0	-2	5
	MVC 4%	1	-2	5
<b>Final limit</b>	MVC 2%	6	0	14
	MVC 3%	4	0	9
	MVC 4%	3	0	7

Tab. 11. ISM error distribution vs MVCs, statistical data.

#### 4.1.4 Discussion of results

##### *Temporal smoothing approach*

Taking into account only temporal data is useful in order to avoid the higher variability that MUPs can present in amplitude. Looking at the algorithm confusion matrix it is evident that a very low number of solutions are identified as MUs when they are not. The main reason identified as the failure condition is imputable to the estimation of MUPs duration samples, particularly in the cannula zone: both the relative threshold and the noise applied to the data can, in some spatial positions, prevent from finding the MUP limits. The classification of mark 2 signals has a very high yield in fact, almost all the solutions are correctly identified as true. Mainly, the failures occur when traces have a small length or when the MU territory is positioned next to the signal edges.

Moreover, the estimations present some overestimation in the initial point and some underestimation in the ending point, with a limited number of outliers.

MVC does not provide significant changes on estimation but, a slight bias of the box plots can be observed reflecting the same behavior of the overall dataset.

The choice of the smoothing parameter needs attention. Despite the Bayesian estimation performed by the function *smoothdiscrepancy*, that provides a compromise between following the data and maintain a low variability of the calculated curve, the smoothing parameter need to be set manually. Its automatic calculation, based on the minimization of the discrepancy coefficient, cannot be properly performed: the variance of the noise present in the signal is not constant. In particular, data variability in the cannula zone is higher than that in the MU territory, and an abrupt change separates them in the transition zone. Hence, in order to improve more the performance, more prior information needs to be obtained before applying this algorithm.

Analyzing the implemented function, it is also possible to notice that when a MU is correctly identified, also its fractions are highlighted. With a refined pecks identification, it may be possible to extract information about their location and length (Fig. 26).

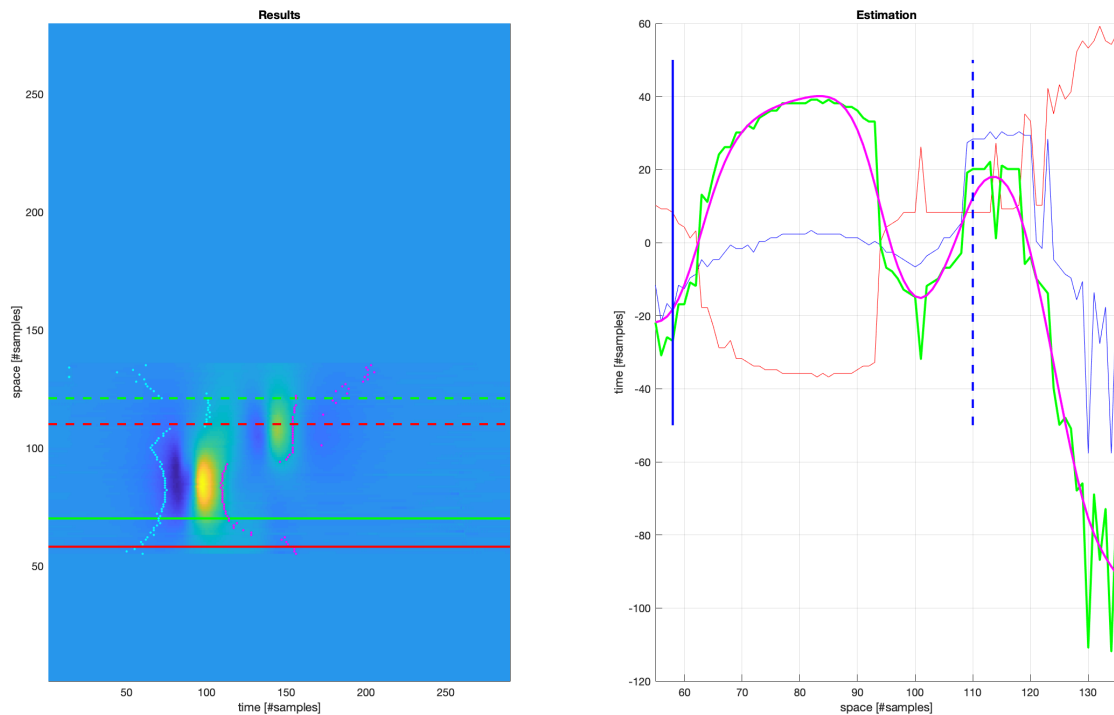


Fig. 26. Example of fraction highlighting on TSA. The positive hills (magenta) represent the two different contributions.

### Differential Amplitude analysis

The analysis of the spatial-amplitude projections takes the advantage from a most representative characterization of the MUP shape. In fact, the MU territory is clearly identifiable in the zone in which a high positive hill occurs. The cannula zone instead, is featured by a constant value inversed polarization.

Results provide, for the parameters chosen, a 100% of identification of those solutions that are marked with 0 (no ground truth overlapping condition). For cases set on 2, the percentage of error is very low and concentrated majorly on the solutions with a low number of traces. In fact, if the record is short, the amplitude projection will be almost constant. Consequently, the derivative component does not present considerable peaks, so they will be undetectable with the set threshold. A possible solution to prevent this issue is through a previous analysis on the amplitude value over the solution: if this remains almost constant, and over a certain amplitude level, the inspected record can be identified as a MU. In this case, estimated limits can be chosen as the ones of the solution itself.

In solutions marked as 2, the error in both the initial and ending points estimation is distributed close to zero but show an under- and an overestimation tendency respectively. These behaviors can be related to the width calculation of the main peak.

Finally, the case 2 signals can be separated and studied as a function of their MVCs. The box plots confirmed the tendencies described before and show, in general, a narrower distribution in the initial



point estimation. Also, a change in MVC does not perturb in a significant way the results making the errors strong respect to the noise applied.

### *Image Segmentation method*

Treating every scanning-MUP as an image it is possible to apply 2D image processing techniques. The algorithm is simple to implement, does not require a large number of instructions and the results obtained are promising.

The algorithm can successfully discard all the traces marked as 0 and provides a very limited error in cases 2 estimation. In this case, the failures occur mainly with solutions composed by a small number of traces.

Looking at the histograms, cases 2 errors are maintained next to the zero-value showing a little under and overestimation tendency respect to the initial and final points to be determined. Although, the overall starting point of the territory is more unbiased and better estimated than ending point. This behavior can be related to the active contour method applied: its main aim is to refine the initial mask, obtained with a thresholding, extending it to a smoothed shape until it matches to some slope characteristics of the MU's positive hill. In particular, the initial limit is usually located in a steeper location than the ending one. Hence, the active contour function can estimate more accurately the transition between cannula and MU territory.

Box plots shows that the algorithm is not influenced by MVC, so by increasing noise. As previously said, the initial point estimation is more accurate and unbiased, when compared to the one done at the end of the territory.

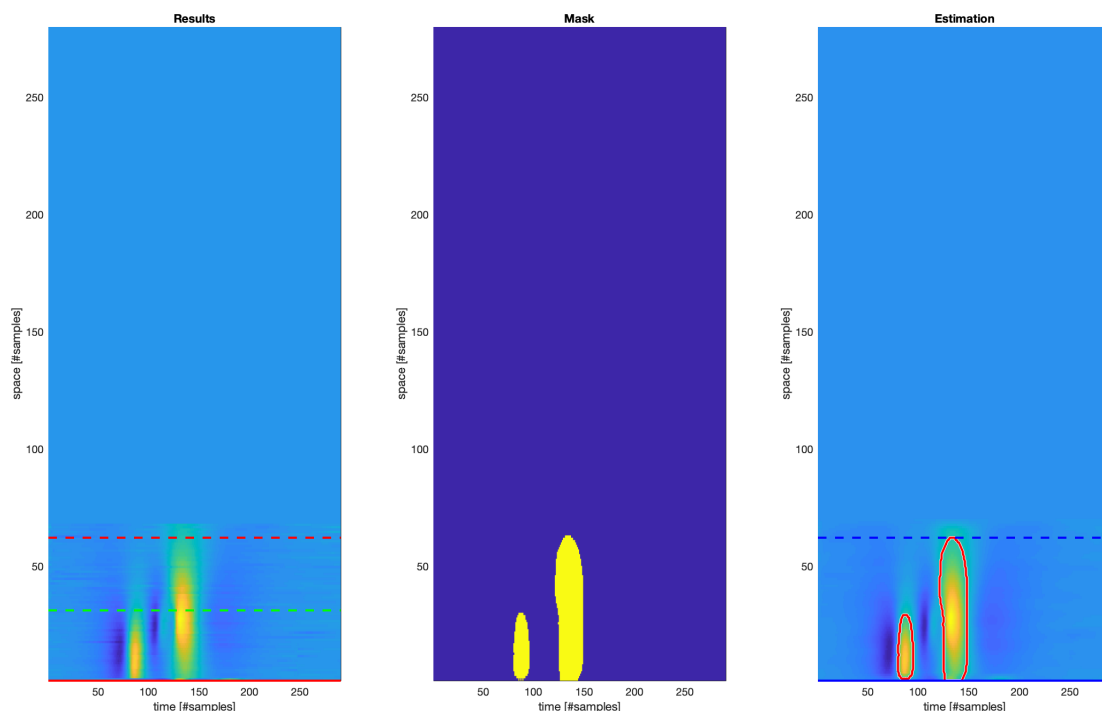


*Fig. 27. Example of fraction highlighting on ISM. The two contribution are segmented individually and masked.*

Another advantage of this technique is that it is possible to identify MU fractions. The initial thresholding can segment multiple zones of the image corresponding to the highest amplitude values.

Next, the active contour algorithm reshapes the detected areas and finally more than a fraction is extracted. In these cases, limits are taken automatically by the algorithm in the same way as presented in chapter 3.2.3.

## 4.2 General results

In this section, a summary of the individual results is made in order to compare between the three different methods. Only those solutions classified as representative of MU territories are considered. So, distribution of errors individually analyzed with histograms in 4.1 are now displayed together in box plots, for the initial and the ending points estimated.

### 4.2.1 Initial limit estimation

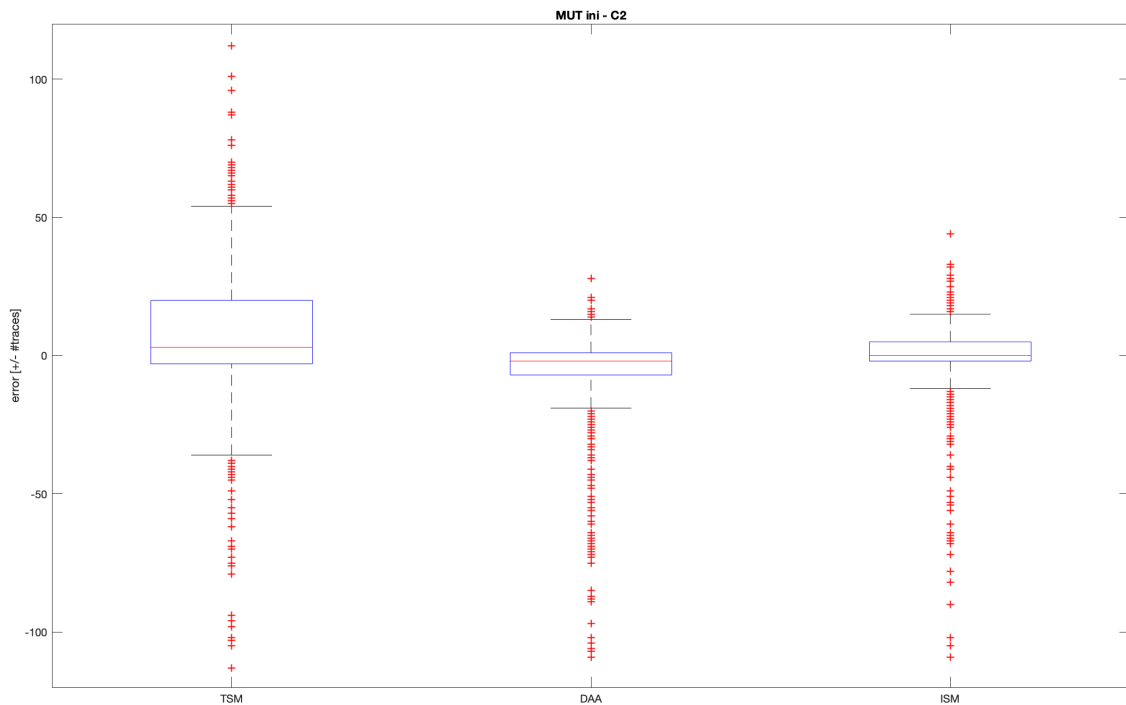


Fig. 28. Error distributions comparison between the three algorithms for the initial MU territory point.

<i>Statistical data [# traces]</i>					
	Mean	Standard deviation	Median	25 <sup>th</sup> percentile	75 <sup>th</sup> percentile
<b>TSA</b>	6.6943	25.4368	3	-3	20
<b>DAA</b>	-6.5719	20.5127	-2	-7	1
<b>ISM</b>	-0.2150	12.7105	0	-2	5

Tab. 12. Summary of method distributions in initial MU territory point, statistical data

## 4.2.2 Ending limit estimation

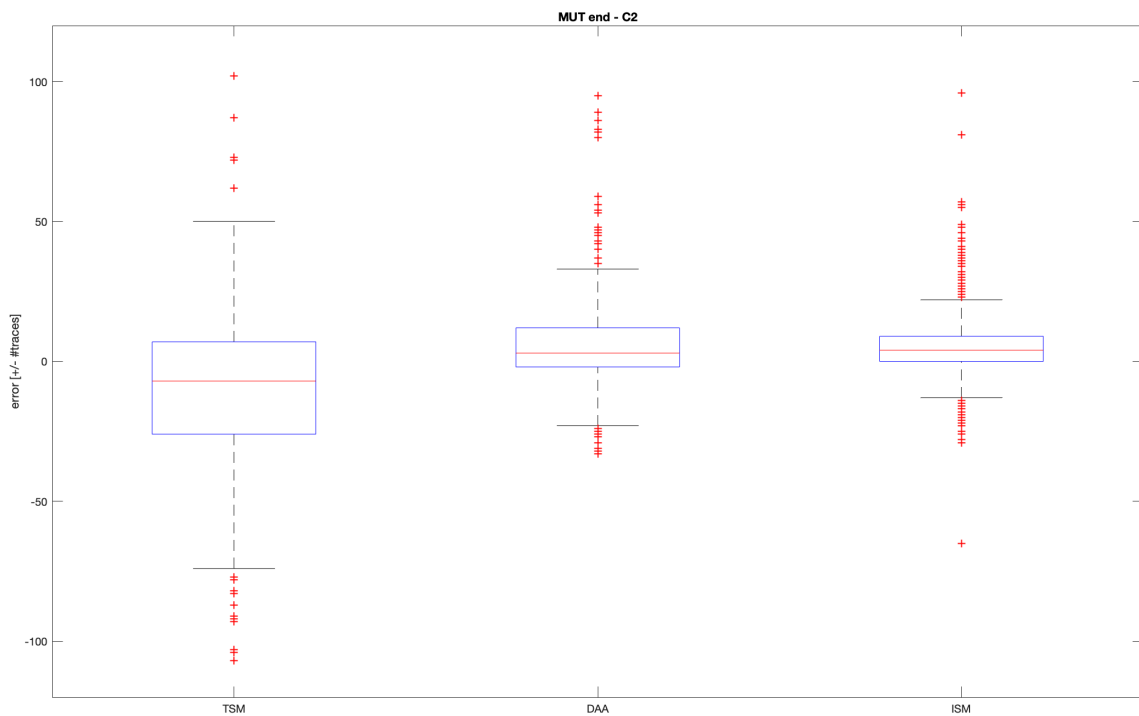


Fig. 29. Error distributions comparison between the three algorithms for the ending MU territory point.

<i>Statistical data [# traces]</i>					
	Mean	Standard deviation	Median	25 <sup>th</sup> percentile	75 <sup>th</sup> percentile
<b>TSA</b>	-10.6852	27.7836	-7.5	-26	7
<b>DAA</b>	5.0477	12.8675	3	-2	12
<b>ISM</b>	5.6509	11.4027	4	0	9

Tab. 13. Summary of method distributions in ending MU territory point, statistical data

## 4.2.3 Discussion of results

All the algorithms proposed achieve the objective of classification scanning-MUP signals as representative of MU territories. The most efficient method is ISM, followed by TSA.

Both ISM and DAA can correctly classify all the scanning-MUPs positioned outside of the ground truth limits. Also, TSA reach a very good level of identification.

TSA can be identified as the less performant method in terms of errors dispersion and present an overestimation tendency in the initial point calculation and an underestimation in the other one. Instead, DAA and ISM show almost the same result behaviors. Both present a tendency to under and overestimate in an opposite way than TSA. The error distributions are narrower and less biased in ISM than the other.

All of the three algorithms proposed are parameter dependent. A different choice of them can drastically reduce, or maybe raise, the percentage of success. In this work, after several tests, algorithms were set up with the best combination of parameters found, by trial and error.

The Kruskal-Wallis test was used in order to find statistical differences between the error distributions of the three implemented methods. The obtained p-values (initial point:  $9.0283e-77$ , ending point:  $1.0379e-90$ ) allow to completely reject the null hypothesis. Also, do not exist statistical similarity in a pair comparison between algorithms (Fig. 30). This behavior can be related to the number of outliers and to the dimensions of data.

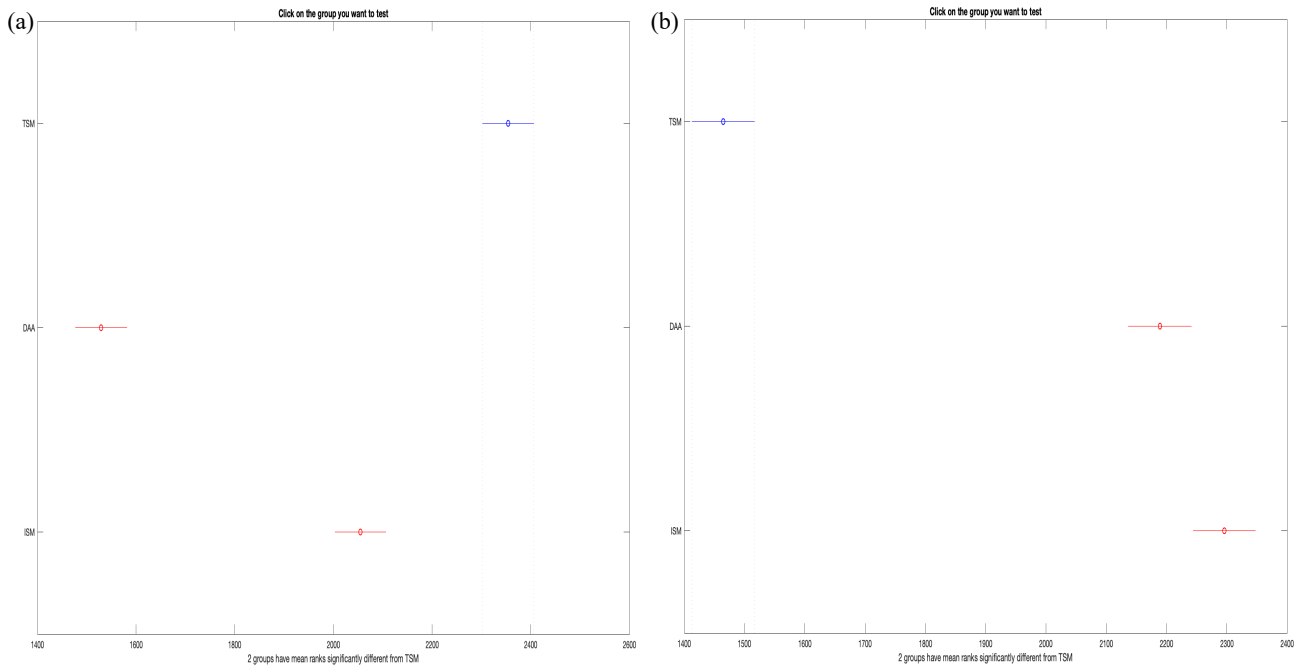


*Fig. 30. Statistical analysis between the three algorithms. No statistical similarity is found between each method and the others. (a) initial point, (b) ending point.*

Taking into account the information in confusion matrices, ISM can be selected as the most performing algorithm. Besides, it possesses two main advantages: the possibility to discriminate fractions and the easier implementation.

# 5 Conclusions and future trends

## 5.1 Conclusions

The main objective of this work was to design algorithms to estimate the active region of the MUs in scanning-MUP signals. These were provided in a wide database created by multiscanning EMG simulations and their corresponding ground truth references, also simulated by a specific MU model. Moreover, three sub-sets of signals were available in according to the MVC levels.

In order to analyze the data and results, two main objectives were accomplished:

- The identification procedure allowed to make a correspondence between simulated solutions and ground truth limits.
- Classifying the degree of overlapping between a solution and reference limits was possible to discard those signals not available for the estimate errors calculation.

Three method were proposed and tested to solve the initial objective: smoothing approach, differential amplitude analysis and image method segmentation. Summarizing the results:

- Stability of the algorithms from signal artifacts.
- Capability to reject solutions marked as 0, not representative of a MU territory. In particular DAA and IMS reach the 100% of success and more of 95% for TSA.
- Solutions marked as 2 are almost all correctly classified by IMS and TSA. Also, DAA provide a very good degree of identification.
- In all the three cases the errors occur majorly in those solutions with a small number of traces.
- Errors seems to be not correlated to changes in MVC, except for a quite low increment of bias in TSA.
- Estimation error distributions show that TSA is the method with a higher variability and bias than the others two. DAA and ISM behavior is very similar but the image-based one seems to be the most precise and accurate.
- Both DAA and ISM present an underestimation and an overestimation tendency in the initial and the ending points respectively. Instead, TSA shows an overturned behavior.
- Each algorithm is found not statistically similar between the others in both initial and ending point estimations.
- TSA allows to highlight MU's fractions. ISM does the same, but their characteristics extraction is immediate through the mask calculation.
- ISM is the easiest algorithm to implement, respect the other two.
- From the above, ISM can be selected as the best method from the ones proposed.

Finally, but not less important, in order to understand the failure conditions of the algorithms and provide an easy way to set their parameters a set of inspection functions were implemented, as described in 3.3.

## 5.2 Future trends

### 5.2.1 Independent ending limit estimation

All the proposed algorithms are mainly focused on the estimation of the cannula-MU territory transition. The upper limit, although well detected, it is been usually estimated applying a dual version of the procedure. Looking at the results, and from the knowledge of the ground truth behavior, a better and independent version of this calculation could be derived.

After the identification of a valid solution, also the maximum amplitude value can be found and, usually, it will correspond to the peak of the positive hill of the MU territory. From this, a relative threshold can be selected or, better, a hard amplitude limit can be taken, e.g. 1mV. Rising to the surface of the muscle along the corridor, the ending limit can be taken as the first position in which the amplitude goes below the established bound.

### 5.2.2 Pattern analysis

The function *scanning\_profile* gives as output the point tracked MUPs turns' lines in two projection, the space-amplitude and the space-temporal ones. In the second case it is simple to see that a change in positive(P)-negative(N) pattern occurs in correspondence of the cannula-MU territory transition. In other words, scanning the traces trough spatial domain, it is possible to identify that: cannula zone follows a P-N-P pattern due to its negative peaks contribution instead the MU territory is characterize for a N-P-N pattern, dual to the previous case.

A change from the pattern PNP to NPN could easily be interpreted as a cannula-MU territory transition but, some issues found during the algorithm implementation can occur and are summarized here in points:

- Construction of the matrix to be analyze: the traces are stored in two different matrices, depending on their sign, occupying a certain spatial location. The idea was to create a single matrix filling every row alternating P and N lines, depending on their occurrence in time. But, the merging of these information could not to be easy to implement due to the possible temporal overlapping between some trace sections.
- Fragmentation of lines: if the previous step can be fixed, the data matrix will be composed by a number of rows dependent on the number of positive and negative tracks. Although, it is possible that lines, due to the noise, can be fragmented in multiple pieces, also separated in space from each other. This behavior can increase the complexity during the reading of the patterns.
- Patterns variability: in the simplest case, cannula and MU territory are characterized by a triplet pattern. In most of the cases other patterns can be found. For example, 'holes' in data matrix can reduce the pattern to a PN or NP duet or, in the other hand, the presence of a fraction can extend the read pattern.

All these factors variability prevented the final implementation of a pattern-based algorithm. It is true that if a stable solution can be found, also this approach can produce good results due to the specificity of the transition from cannula to MU territory.

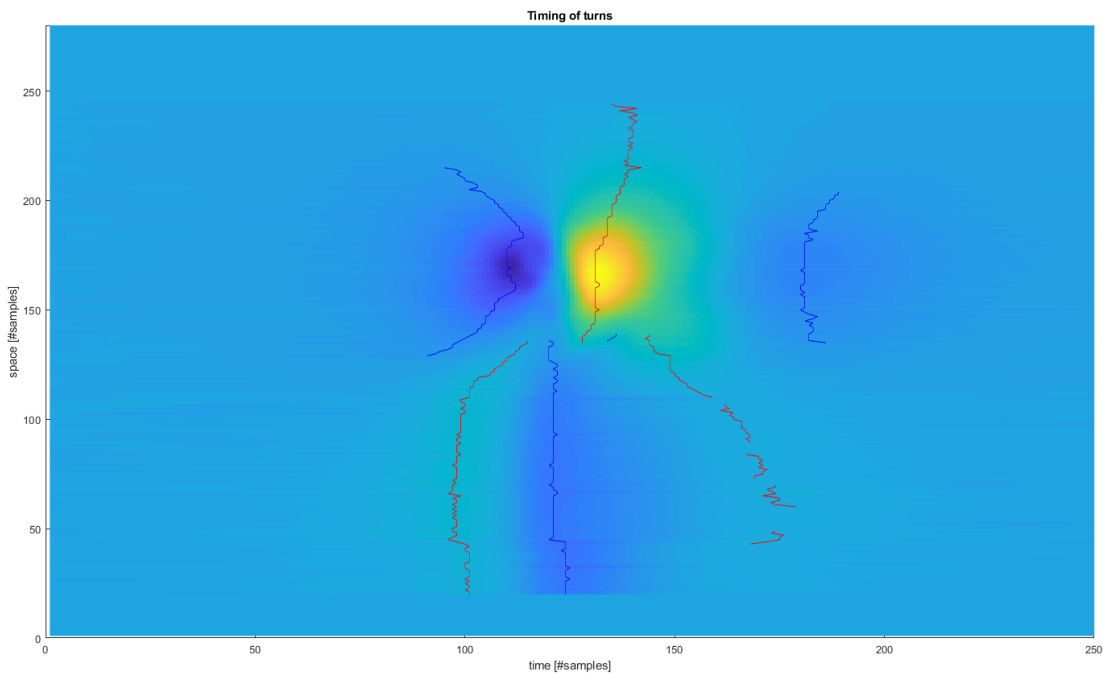


Fig. 31. Example of turns pattern, positive (P) in red and negative (N) in blue.

### 5.2.3 Mask generation

Once the spatial limits are determined, the data scanning-MUP matrix can be masked, retaining only the MU territory information. In order to do that, temporal duration of the recorded MUPs has to be determined. The absolute threshold for the calculation of these values seems to be, at a first look, the most effective and representative. After this selection, the Q-EMG description could be easily performed.

### 5.2.4 Real cases analysis

Simulation data are very useful during the algorithms setting. Nevertheless, real signals are the ones in which a possible future implementation of these methods must perform as well as possible.

On real data analysis, for example, the superimposed noise can be higher and the presence of artifacts can make harder both the recordings and the subsequent estimations. Also, in the database used in this Thesis, pathological conditions are not simulated, such as neuropathies or myopathies, that introduce new source of variability that may affect the estimation techniques.

In conclusion, starting from the positive results previously presented, algorithms need to be tested on real data in order to be refined and optimized.





# Bibliography

- [1] I. Carreño Rodríguez, *Cancellation of baseline fluctuation in electromyographic signals and measurement of motor unit action potential duration based on wavelet transform*, Diss. Universidad Pública de Navarra, 2006.
- [2] B. R. MacIntosh, P. F. Gardnier and A. J. McComas, *Skeletal muscle: form and function*, Human Kinetics, 2006.
- [3] J. Navallas, J. Rodríguez and E. Stålberg, "Scanning electromyography," in *EMG Methods for Evaluating Muscle and Nerve Function*, IntechOpen, 2012.
- [4] T. Adel and D. Stashuk, "Clinical quantitative electromyography," in *Electrodiagnosis in New Frontiers of Clinical Research*, IntechOpen, 2013.
- [5] N. T. Artuğ, İ. Göker, B. Bolat, M. B. Baslo and O. Osman, "Determining MUAP activity corridor in scanning EMG recordings," *2015 International Symposium on Innovations in Intelligent SysTems and Applications (INISTA)*, 2015.
- [6] I. Corera, A. Eciolaza, O. Rubio, A. Malanda, J. Rodríguez-Falces and J. Navallas, "A masked least-squares smoothing procedure for artifact reduction in scanning EMG recordings," *Medical & biological engineering & computing*, 2018.
- [7] I. Corera, A. Malanda, J. Rodríguez-Falces, S. Porta and J. Navallas, "Motor unit profile: a new way to describe the scanning EMG potential," *Biomedical Signal Processing and Control*, 2017.
- [8] A. Ferrando Eciolaza, *Multiscanning-EMG con una aguja*, Universidad Pública de Navarra, 2018.
- [9] J. P. Van Dijk, U. Eiglsperger, D. Hellmann, N. N. Giannakopoulos, K. C. McGill, H. J. Schindler and B. G. Lapatki, "Motor unit activity within the depth of the masseter characterized by an adapted scanning EMG technique," *Clinical Neurophysiology*, 2016.
- [10] T. F. Chann and L. A. Vese, "Active contours without edges," *IEEE Transactions on image processing*, 2001.



# Figures index

FIG. 1. SCANNING EMG SYSTEM (EXTRACTED FROM [3]).....	8
FIG. 2. SCHEMATIC REPRESENTATION OF A SCANNING EMG PROCEDURE (EXTRACTED FROM [3]).....	9
FIG. 3. MUP AS LEVEL MAP. ON THE RIGHT THE REPRESENTATION OF THE SIGNALS IN CHARACTERISTIC LOCATIONS (EXTRACTED FROM [3])...	10
FIG. 4. EFFECT OF SPATIAL FILTERING. (A) RAW SIGNAL. (B) APPLICATION OF A 7-POINTS MEDIAN FILTER. (C) APPLICATION OF THE LEAST-SQUARE BASED FILTER. (D) IDEAL NOISE FREE MUP (EXTRACTED FROM [6]). .....	12
FIG. 5. REPRESENTATION OF MUP PROJECTIONS. THE SOLID LINES CORRESPOND TO POSITIVE LINKED TURNS, THE DOTTED ONES TO THE NEGATIVES. THE CORRESPONDENCE BETWEEN LINES IS GIVEN BY THE NUMBERS. (A) SPACE-AMPLITUDE PROJECTION. (B) SPACE-TIME PROJECTION (EXTRACTED FROM [7]). .....	13
FIG. 6. SCHEME OF MULTISCANNING-MUP RECORDING. (A) EEG RECORDED FOR EACH POSITION BY THE NEEDLE ELECTRODE. (B) MUP DECOMPOSITION FOR EACH POSITION DEPENDING ON DIFFERENT MUS. (C) MUP GENERATION BY LINKING PROCEDURE (EXTRACTED FROM [8]). .....	14
FIG. 7. ESTIMATION OF MU TERRITORY GROUND TRUTH LIMITS. (A) FIBERS CONTRIBUTION. (B) NO FIBERS CONTRIBUTION. ....	18
FIG. 8. SCHEMATIC REPRESENTATION OF MARKING PROCEDURE. SOLUTION LIMITS ARE REPRESENTED WITH THE BLACK LINES. THE MU GROUND TRUTH TERRITORY IS REPRESENTED FOR FIBERS/NO FIBERS CONTRIBUTIONS IN GREEN AND YELLOW RESPECTIVELY. IN SHADOWED BLUE IS REPRESENTED AN APPROXIMATED RECORDING CAPTION AREA. (A) MARK 0, (B) MARK 1, (C) MARK 2.....	19
FIG. 9. SCHEME OF THE SOLUTIONS MARKING ALGORITHM. ....	20
FIG. 10. SCHEME OF TSA ALGORITHM.....	22
FIG. 11. TSA ESTIMATION. ON THE RIGHT: DURATION DATA (BLUE AND RED), THEIR SUBTRACTION (GREEN), SMOOTHING (MAGENTA) AND LIMITS (BLUE). ON THE LEFT: SOLUTION WITH DURATIONS DATA (CYAN AND MAGENTA), GROUND TRUTH (GREEN) AND ESTIMATION (RED).....	23
FIG. 12. SCHEME OF DAA ALGORITHM.....	25
FIG. 13. DAA ESTIMATION. AMPLITUDE PROFILE DATA (BLUE AND RED), THEIR DERIVATIVE COMPONENTS (GREEN AND MAGENTA). ....	26
FIG. 14. SCHEME OF ISM ALGORITHM. ....	27
FIG. 15. ISM ESTIMATION. ....	28
FIG. 16. EFFECT OF THE 2D FILTER. ON THE RIGHT IS REPORTED THE FILTERED VERSION OF THE SOLUTION ON THE LEFT. ....	29
FIG. 17. TSA ERROR DISTRIBUTION. ....	33
FIG. 18. TSA RELATIVE ERROR VS LENGTH OF THE SOLUTION. ....	34
FIG. 19. TSA ERROR DISTRIBUTION ERROR VS MVCs. ....	34
FIG. 20. DAA ERROR DISTRIBUTION. ....	36
FIG. 21. DAA RELATIVE ERROR VS LENGTH OF THE SOLUTION. ....	37
FIG. 22. DAA ERROR DISTRIBUTION VS MVCs. ....	37
FIG. 23. ISM ERROR DISTRIBUTION.....	39
FIG. 24. ISM RELATIVE ERROR VS LENGTH OF THE SOLUTION.....	40
FIG. 25. ISM ERROR DISTRIBUTION VS MVCs.....	40
FIG. 26. EXAMPLE OF FRACTION HIGHLIGHTING ON TSA. THE POSITIVE HILLS (MAGENTA) REPRESENT THE TWO DIFFERENT CONTRIBUTIONS. ....	42
FIG. 27. EXAMPLE OF FRACTION HIGHLIGHTING ON ISM. THE TWO CONTRIBUTION ARE SEGMENTED INDIVIDUALLY AND MASKED.....	43
FIG. 28. ERROR DISTRIBUTIONS COMPARISON BETWEEN THE THREE ALGORITHMS FOR THE INITIAL MU TERRITORY POINT. ....	44
FIG. 29. ERROR DISTRIBUTIONS COMPARISON BETWEEN THE THREE ALGORITHMS FOR THE ENDING MU TERRITORY POINT. ....	45
FIG. 30. STATISTICAL ANALYSIS BETWEEN THE THREE ALGORITHMS. NO STATISTICAL SIMILARITY IS FOUND BETWEEN EACH METHOD AND THE OTHERS. (A) INITIAL POINT, (B) ENDING POINT. ....	46
FIG. 31. EXAMPLE OF TURNS PATTERN, POSITIVE (P) IN RED AND NEGATIVE (N) IN BLUE.....	49



# Tables index

TAB. 1. MODELS PARAMETERS AND VALUES [8]. .....	16
TAB. 2. COMPOSITION OF THE DATABASE. ....	31
TAB. 3. TSA CONFUSION MATRIX. ....	33
TAB. 4. TSA ERROR DISTRIBUTION, STATISTICAL DATA.....	33
TAB. 5. TSA ERROR DISTRIBUTION VS MVCs, STATISTICAL DATA.....	35
TAB. 6. DAA CONFUSION MATRIX. ....	36
TAB. 7. DAA ERROR DISTRIBUTION, STATISTICAL DATA.....	36
TAB. 8. DAA ERROR DISTRIBUTION VS MVCs, STATISTICAL DATA.....	38
TAB. 9. ISM CONFUSION MATRIX. ....	39
TAB. 10. ISM ERROR DISTRIBUTION, STATISTICAL DATA .....	39
TAB. 11. ISM ERROR DISTRIBUTION VS MVCs, STATISTICAL DATA. ....	41
TAB. 12. SUMMARY OF METHOD DISTRIBUTIONS IN INITIAL MU TERRITORY POINT, STATISTICAL DATA.....	44
TAB. 13. SUMMARY OF METHOD DISTRIBUTIONS IN ENDING MU TERRITORY POINT, STATISTICAL DATA .....	45